

Alessandro Baratta¹, Ottavia Corbi²

The static behavior of historical vaults and cupolas

Zachowanie statyczne historycznych sklepień i kopuł

Keywords: Masonry behaviour, Masonry vaults, Structural assessment, No-Tension model

Słowa kluczowe: statyka elementów murowanych, murowane sklepienia, ocena konstrukcyjna, model beznaprężeniowy

1. INTRODUCTION

Masonry is the main material mankind has exploited to provide itself a shelter.

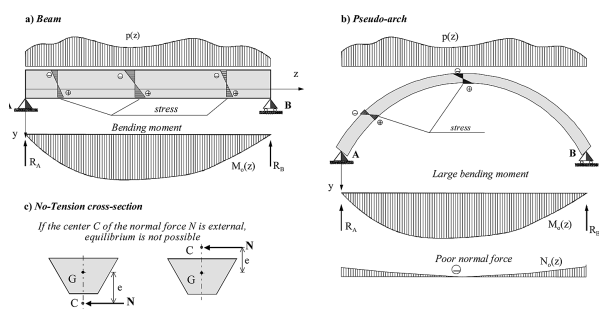


Fig. 1. a) Beam requires compression/tension stresses to be resisted; b) Curvature of the beam does not help by itself to cancel tension; c) If the eccentricity e is large No-Tension equilibrium cannot subsist

Homes, temples, offices, markets and so on are built by some kind of masonry since the beginning of civilization. Walls are the main way loads are transferred to foundations and to underlying soil, but horizontal floor structures require some more skill, since masonry, due to its very poor, unreliable, inhomogeneous and time-degrading, tensile strength, is not able to resist bending moments. This is the reason why masonry buildings are often complemented by wood or, more recently, steel systems to cover spaces, providing beam elements resisting by pure flexure.

In a simply supported beam, equilibrium is sustained by bending moments, which in turn require that compression stresses are coupled with tension (Fig. 1a); so if some beam has ever been attempted it is soon realized that failure is inexorable.

On the other side, early ante-literam architects learned from nature that it is possible to overpass empty spaces by stones: natural arches are encountered everywhere in the world (Fig. 2).



Fig. 2. Natural Arches: a) Capri (Italy); b) The "Elephant Arch" in Pantelleria (Italy)

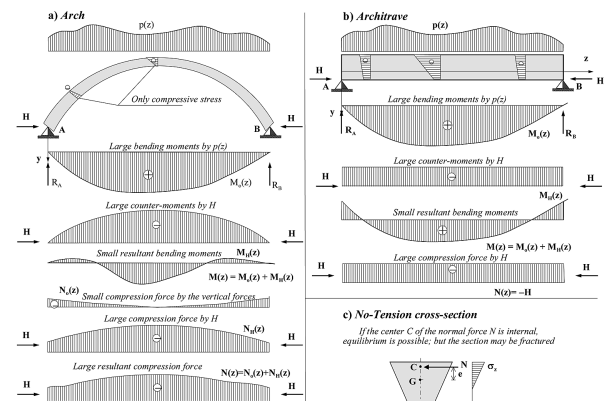


Fig. 3. a) True arch: the action of the thrust force H increases the normal force and mitigates the bending moment. A small eccentricity $e = M/N$ results; b) The same happens for a beam with horizontally contrasted supports, thus resulting in an architrave; c) The eccentricity is small and the center C of the normal force is in the interior of the cross-sections

So, the first character that is acquired at glance is that the masonry should be "curve". If one consider a curved beam (the pseudo-arch in Fig. 1b) one finds that the only difference is the insurgence of a compressive normal force on the cross-section, which mitigates, but does not cancel, the need for tension (Fig. 1b). The bending moments remain the same, the normal force is small, the eccentricity is large and the center of the force is

¹ Full professor, University of Naples „Federico II”, Italy, Dept. of Struct. Eng.ng, email: alebarat@unina.it

² Assoc. professor, University of Naples „Federico II”, Italy, Dept. of Struct. Eng.ng, email: corbi@unina.it

generally out of the cross section (Fig. 1c): equilibrium cannot subsist unless tension is resisted where it is necessary in the structure. If the system is horizontally fixed at both ends, a new entity is born, the *horizontal thrust H*, which drastically changes the static regime and a true *arch* is realized. The thrust force is the key for the arch statics. It acts, in fact, producing larger compressive normal forces and strong counter-moments (Fig. 3a), thus mitigating the flexure and enhancing compression. The effect is quite independent on apparent curvature: the important fact is that a horizontal force exists able to produce counter-moments with respect to active load. The architrave is nothing else than an arch with the appearance of a beam (Fig. 3b). The typical condition is a composite compression-flexure stress, where the compression is large and the flexure is small, so that the eccentricity with respect to the central line is strongly reduced and the center of force enters in the interior of the cross section: equilibrium is now possible by purely compressive stresses (Fig. 3c).

So, Man learned that it was possible to cover spaces with stones. Anyway, he found and inhabited also large caves, so the attempt to reproduce nature (a strong impulse in Architecture, as testified also in recent times by the Gaudi's opera, see e.g. [1]) may be has pushed to realize double-curvature roofs. This activity gradually resulted in a success, with larger and larger spans being covered, thus leading to the early architecture and to its developments up to our times.

The historical development of Structural mechanics is exhaustively reconstructed in the book by E. Benvenuto [2]. A very interesting and complete historical survey on the conception, realization and progress in the masonry vaults technology can be found in [3] and in [4, 5]. Here an observation by Thomas Young is reported, namely: "*The construction of the dome is less difficult than that of an arch since the tendency of each arch to fall is counteracted not only by the pressure of the parts above and below but also by the resistance of those which are situated on each side.....*". That double curvature surfaces are easier to be built than simple arches or barrel vaults is a fact that will receive further specification in the sequel.

2. THE MASONRY AS A MATERIAL

2.1. Overall properties

Masonry is not properly a "material" in the strict sense of the word. It consists in the (generally man-made) assemblage of a basic component (the stones) simply laid on each other or, more often, jointed by mortar. Stones and mortar may have very variable mechanical properties, and the way in which the stones are organized in the masonry volume may (the masonry "texture") may be very different, and is subject to the skill and the creativity of the designer and/or of the builder.

So, "masonry" has not a uniquely defined object, and it is very difficult to set up a mechanical model able to closely reproduce the properties of masonry, fitting all the possible variety of masonry assortment and texture.

Anyway, in all structural analyses the engineer is forced to balance the trend to reproduce the material (and consequently the structural behaviour) as closely as possible, with the practical manageability of the analytical tools. Linear theory of structures applied to steel, reinforced concrete and even to masonry, is a successful example of such effort. In all cases the basic theory should include the major features of the behaviour, possibly neglecting many details that poorly influ-

ence structural safety assessment, and/or are uncontrollable. The small tensile strength in concrete, for instance, not only yields a poor contribution to the structure performance, but since it is a highly uncertain parameter in the concrete mass of a building, it increases uncertainty of the analysis' results: so it is preferred to adapt linear theory by neglecting tensile strength rather than to exploit cumbersome procedures yielding results depending on uncontrollable parameters.

The first step is then to identify the major properties, that are more or less common to all masonry types. The basic knowledge can be achieved through simple experiments. Uni-axial compression/tension tests can be performed on some Representative Volume Element (RVE) of a typical masonry (Fig. 4).

After some experiments, it is possible to conclude that (Fig. 4a): i) the masonry has different elastic moduli in tension (E_t) and compression (E_c); ii) the masonry has different limit stresses in tension (σ_t) and compression (σ_c); iii) the limit stress in tension is much smaller than the limit strength in compression ($\sigma_t \ll \sigma_c$); iv) the behaviour at failure in compression has some degree of ductility; v) the behaviour at failure in tension is definitely brittle, so tensile strength cannot be recovered absolutely.

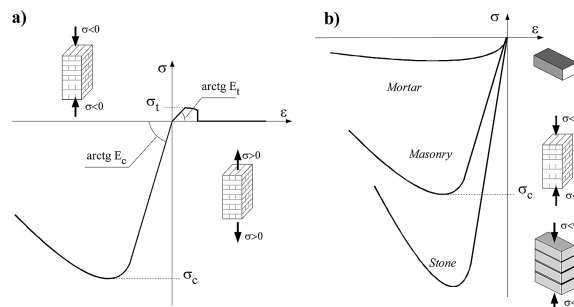


Fig. 4. a) A typical test of compression/tension on a masonry specimen; b) The limit strength in compression is intermediate between the strength of mortar (small) and the strength of the bricks (large)

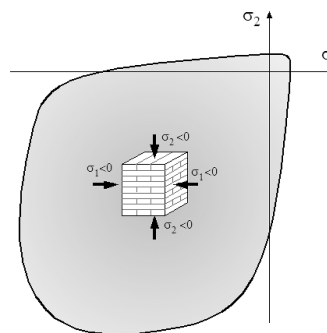


Fig. 5. Synthesis of biaxial tests on masonry prisms. Limit domain (see e.g. Hegemier [6] and Page [7])

Moreover, surprisingly (Fig. 4b), the limit strength in compression of masonry is larger than the strength of the weak element (the mortar) and is bounded from above by the limit strength of the strong component (the stones); this is due to some complex phenomenon of stress interaction and transverse deformation of mortar with respect to stones. It is also easy to understand that if the axis of the stress is rotated by an angle, say 90° , the results of the experiment may significantly change, in particular as regards the tensile strength. Some similar conclusions can be drawn from biaxial tests (see e.g.

[6, 7]). Experimental limit strength domains are of the type in Fig. 5, showing a high capacity in compression and a very poor limit in tension without ductility.

Summing up, masonry is a non-linear material, strongly hetero-resistant, anisotropic with respect to tensile strength, with compliance coefficients depending on the orientation of the stress axes and different in compression and tension, and with brittle failure at the tension threshold.

2.2. Influence of the texture on masonry properties. The case of the masonry wall

The influence of the texture on the masonry performance can be illustrated by the following example. Assume that a panel is built by regular bricks with interposed poor mortar joints, lacking any adhesive power. Consider that bricks are set according to the following two patterns (Fig. 2.3a and 2.3b)

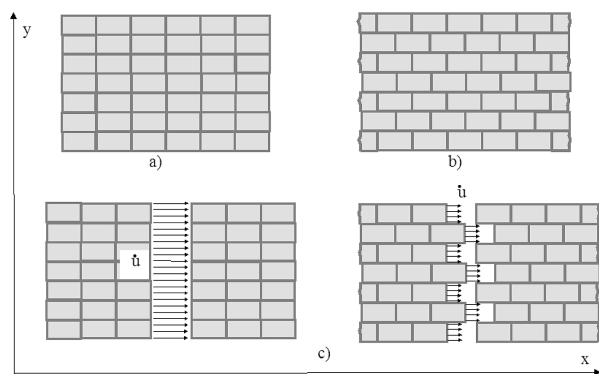


Fig. 6. Masonry element: a) Aligned bricks; b) Staggered bricks; c) Free lateral expansion for both panels

If there is no vertical compression both panels are free to expand laterally without encountering any resistance (Fig. 6c).

If a vertical compression is applied, the panel in Fig. 6a still can freely separate; by contrast an horizontal tensile pseudo-strength becomes active in the panel in Fig. 6b, because of friction and interlocking of bricks with each other. The failure mechanism in Fig. 7b can be studied for the bi-dimensional masonry plane element in Fig. 7a having a friction coefficient f , a joints stagger s (Fig. 7c) and a row density ω defined as the ratio between the number of block rows in the panel height H and the height H . In Fig. 7 $\omega = 7/H$.

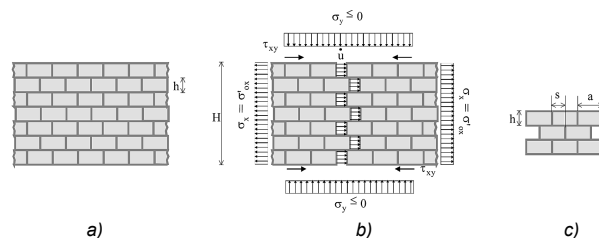


Fig. 7. Masonry element: a) Geometrical dimensions, b) Failure mechanism under compression and limit tensile forces, c) Stagger parameter

The wall is subjected to vertical compression stresses σ_y orthogonal to the joints direction and horizontal tractions σ_x parallel to the joints. It is possible to prove [8] that the horizontal tensile strength σ'_{ox} is given by (Fig. 7b)

$$\sigma'_{ox} = -f\sigma_y s\omega \quad (1)$$

The ratio between the compressive stress on the joints and the transverse tensile strength is

$$\left| \frac{\sigma'_{ox}}{\sigma_y} \right| = fs\omega \quad (2)$$

If the length of the stone is a , s is of the order $a/2$. Usually $a > 2h$ (very often $a > 4h$), with h the thickness of the brick, and so $s > h$. On the other side, $\omega \approx 1/h$, so that $s\omega > 1$ (very often $s\omega > 2$). With the help of mortar and/or of roughness of the interface between stones, f may possibly be rather large ($f = 0.5 \div 0.8$), and the ratio in Eq. (2) is frequently larger than 1, i.e. the tensile strength in the direction parallel to joints is larger than the acting compressive stress.

It can be also proved that a pretty ductility is associated to the tensile strength σ'_{ox} . With reference to the diagrams in Fig. 8, applying a safety coefficient γ to the limit resistance σ'_o , the loss in strength is balanced by a gain in ductility. In other words if σ'_a is the admissible stress and δ_a is the maximum ductility, one can write

$$\sigma'_a = \sigma'_o / \gamma \quad ; \quad \delta_a = \frac{\epsilon'_{oa}}{\epsilon'_a} = 1 + \frac{\epsilon'_r}{\epsilon'_o} (\gamma - 1) \quad (3)$$

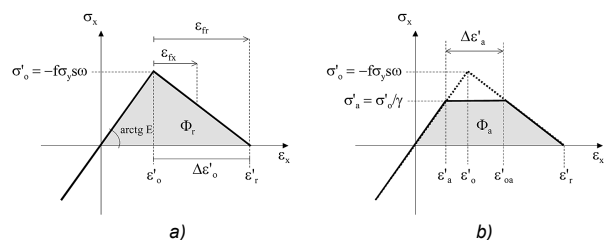


Fig. 8. a) Stress vs. deformation in the tension range, b) conventional diagram with variable ductility

A fundamental observation is that Eq. (1) not only expresses the tensile resistance of the masonry element, but also puts to evidence that the tension can be contrasted in function of the static needs by means of a skilled orientation of the texture of the masonry blocks and of the mortar joints. After recognizing that by the combined effect of compression and friction the lines of the mortar joints are probably the lines where original designers and builders intended to provide tensile strength in the masonry mass, it can be conceived that a technical practice had spread out, very similar to the modern technology of reinforced concrete where the structural designer inserts steel bars in way to balance tension along stretched lines.

Many examples proving that clever architects were aware of this effect when designing vault structures can be illustrated.

3. MASONRY TEXTURE AND APPARATUS IN VAULT STATICS

3.1. The cantilever stairs

In the static analysis of a vaulted staircase, like in Fig. 9, it is possible to recognize three basic typological components: the landings, the angle connections, and the flights of stairs (two or three depending on the structure morphology). The structure is supported by the outside walls system which represents the stairs box.

Looking at the section of a vaulted stair in Fig. 10a, such structural conformation suggests an apparent paradox: despite the fact that masonry is not effective in sustaining tension

stresses and bending, it should work as a cantilever, or however it is an incomplete vault which lacks the counter-thrust from the missing part of the arch (Fig. 10b) and so being prone to lose the equilibrium state (Fig. 10c).

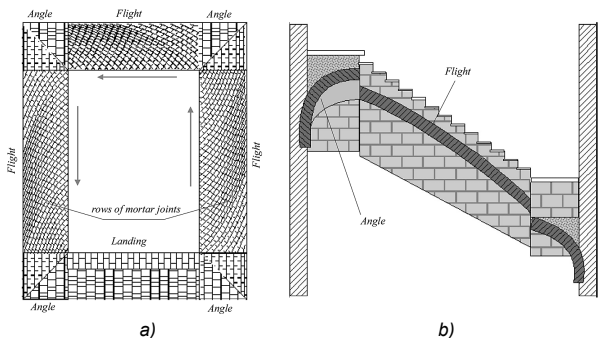


Fig. 9. Vaulted stairs: a) Planimetric view; b) Longitudinal section

It is quite obvious that the solution of the contradiction goes pursued abandoning the search of improbable plane patterns and by investigating three-dimensional equilibrium paths accounting for the space articulation of such structural organisms, searching stress fields in equilibrium and compatible with the resistant abilities of the masonry material as usually interwoven in the case of “cantilever” stairs.

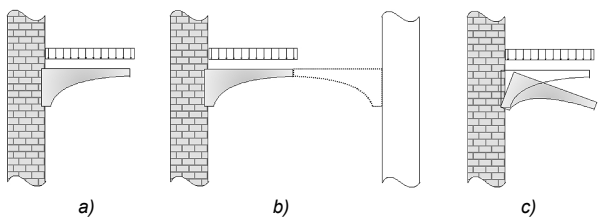


Fig. 10. Transverse sections of vaulted stairs: a) Section and particular of one step; b) “Half barrel vault” model; c) Improbable “cantilever” behaviour

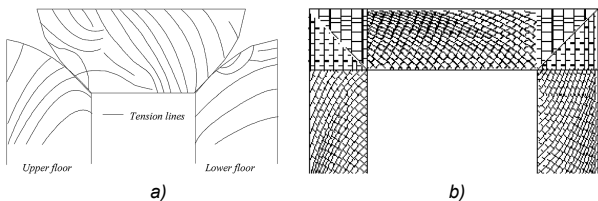


Fig. 11. Comparison of tension isostatic lines with the mortar rows. a) Tension lines calculated by a FEM (linear) procedure; b) Mortar rows in the flights

After identifying the basic internal force distributions through which the stairs can equilibrate their own weight and live loads, and the correlation that was intended by the original builders between statics and masonry tissue, it is also possible to design the reinforcement of the vaults, that shall be designed in way to sustain the possible equilibrium paths. Apart from complex analyses (see e.g. [9]), it is possible to identify simplified equilibrium patterns that are compatible with the load-carrying capacity of the structure [10]. All these approaches, FEM and/or simple 3D-beam, agree in identifying isostatic tension lines that approximately agree with the proceeding of the rows of mortar joints (Fig. 11), that are compressed in the orthogonal direction, thus developing a tension capacity along their lines of action; thus proving that the statics of these stairs are strictly connected with the vault apparatus. It is also possible to use this argument in an inverse fashion,

i.e. to infer isostatic lines proceeding from the observation of the masonry texture. Any double curvature cover, in fact, is a highly hyperstatic system, which means that it can select its own pattern in a large set of possible equilibrium paths. So texture and vault apparatus are a tool by which, apart from the shape of the vault (barrel vault, rib vault, groin vault, etc.) the architect can steer the structure to work in some preferred way.

3.2. Tension in spherical domes

Consider the axial-symmetric hemispherical dome with radius R and thickness t (Fig. 12a), supporting its own weight w , where it is well known that in the classical solution, tension should be active along the parallel lines after some degree of the zenith angle $\varphi = 51.8^\circ$.

Here the meridian stress N_φ and the hoop stress N_θ are [11]

$$\begin{cases} N_\varphi = -\frac{wR}{1 + \cos \varphi} \\ N_\theta = wR \left(\frac{1}{1 + \cos \varphi} - \cos \varphi \right) \end{cases} \quad (4)$$

with $w = \gamma t$ and γ the unit weight of the material constituting the shell.

The ratio is

$$\frac{N_\theta}{N_\varphi} = 1 - \cos \varphi - \cos^2 \varphi \quad (5)$$

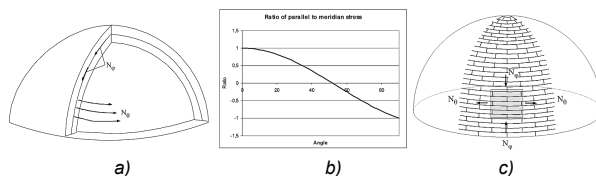


Fig. 12. a) Spherical dome; b) Ratio of parallel to meridian stress resultant. N_j is everywhere compressive for any j , and N_q is a tensile stress for $j > 51.8^\circ$; c) The friction pattern yields a admissible stress if $fsw > 1$

The ratio is plotted in Fig. 12b, whence one can see that the ratio is always not larger than 1. So, if masonry is organized by staggered regular bricks –as often happens– tension could generally be faced by the friction mechanism as illustrated in Sec. 2.2 (Fig. 12c).

Anyway, equilibrium can be found by some other membrane surface other than the mean surface of the shell, provided it is included in the thickness between the (spherical) intrados and extrados. Considering a revolution membrane surface having an elliptic profile with radii a and b , included in the interior of the hemisphere (Fig. 13a) the internal forces equilibrating the weight of the spherical dome can be found by the following procedure

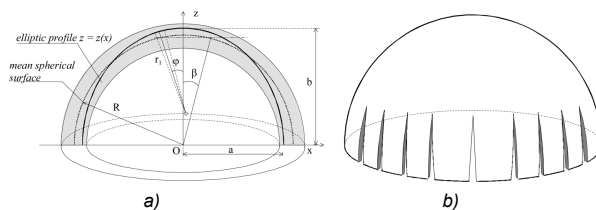


Fig. 13. a) The elliptic membrane surface included in the dome thickness; b) Possible physiological fractures in the masonry

Consider the spherical cap above the center angle β , whose weight is

$$W = 2\pi w R^2 (1 - \cos\beta) \quad (6)$$

The angle β is related to the zenith angle φ by the relationships

$$\sin\beta = \frac{a \sin\varphi}{\sqrt{a^2 \sin^2\varphi + b^2 \cos^2\varphi}} ; \quad \cos\beta = \frac{b \cos\varphi}{\sqrt{a^2 \sin^2\varphi + b^2 \cos^2\varphi}}$$

$$d\beta = \frac{ab}{a^2 \sin^2\varphi + b^2 \cos^2\varphi} d\varphi \quad (7)$$

The radii of curvature of the ellipsoidal surface are ([11], p. 40)

$$r_1(\varphi) = \frac{a^2 b^2}{(a^2 \sin^2\varphi + b^2 \cos^2\varphi)^{3/2}} ;$$

$$r_2(\varphi) = \frac{a^2}{(a^2 \sin^2\varphi + b^2 \cos^2\varphi)^{1/2}} \quad (8)$$

so that

$$\sin\beta = \frac{ar_2(\varphi)\sin\varphi}{a^2} = \frac{r(\varphi)}{a} ; \quad \cos\beta = \frac{b}{a} \frac{r(\varphi)}{a \tan\varphi} \quad (9)$$

$$\text{with } r(\varphi) = r_2(\varphi)\sin\varphi$$

and

$$d\beta = \frac{a}{b} \frac{r_1(\varphi)}{r_2(\varphi)} d\varphi \quad (10)$$

The equilibrium versus the vertical translation can be written

$$2\pi r_2 N_\varphi(\varphi) \sin^2\varphi + W = 0 \quad (11)$$

and

$$N_\varphi(\varphi) = -\frac{wR^2(1 - \cos\beta)}{r_2(\varphi)\sin^2\varphi} \quad (12)$$

The ellipsoidal membrane shall now sustain the weight w of the spherical shell, that transforms in the weight w^* on the ellipsoid setting

$$w^* r_1(\varphi) d\varphi r(\varphi) d\theta = w R d\beta r_s d\theta ; \quad r_s = R \sin\beta \quad (13)$$

whence

$$w^* = w R^2 \frac{1}{b r_2(\varphi)} \quad (14)$$

The equilibrium along the outward normal to the (ellipsoidal) membrane yields

$$\frac{N_\varphi(\varphi)}{r_1(\varphi)} + \frac{N_\theta(\varphi)}{r_2(\varphi)} = p_n(\varphi) = -w^* \cos\varphi = -w \frac{R^2}{b r_2(\varphi)} \cos\varphi \quad (15)$$

and

$$N_\theta(\varphi) = -\left(w \frac{R^2}{b} \cos\varphi + N_\varphi(\varphi) \frac{r_2(\varphi)}{r_1(\varphi)} \right) \quad (16)$$

Ellipsoidal stress surface can be active in order to mitigate tension hoop stresses, possibly after some fractures have opened (Fig. 13b), that can be considered physiological if masonry has some degree of ductility in the parallel direction, as in the friction strength mechanism illustrated in Sec. 2. In Fig. 14a various membrane stress surfaces are plotted, with different ratios a/b . Note that such surfaces make sense provided that they remain included in the thickness of the spherical shell, i.e. if $t \geq 2(R-a)$ and $t \geq 2(b-R)$, with $b \geq a$. The plots in Fig. 14b prove that the ratio of the parallel to the meridian normal force can be mitigated, and also be near 0.4 and smaller, with increasing the ratio b/a . Consider that both in the spherical and in the elliptic membranes, the stress surface is a complete semi-ellipsoid, with $\varphi = 90^\circ$ at $y = 0$, so that the equilibrium solutions do not require any thrust force at the bottom support $y = 0$.

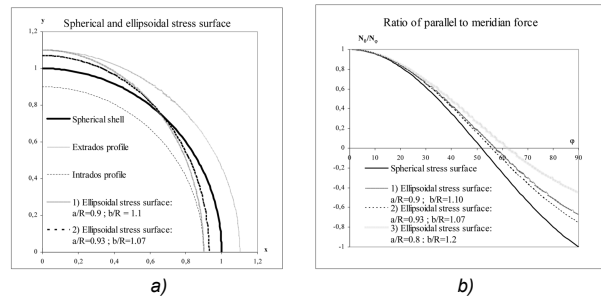


Fig. 14. a) Ellipsoidal membrane surfaces for different ratios of the ellipsoid radii a and b to the radius R of the spherical dome; b) Ratio of N_p to N_t for different shapes of the elliptic profile

Anyway, it has been proved by [12] that a membrane surface included in the thickness of the dome can be found without hoop tension, provided that a adequate counter-thrust force can be exerted at the bottom of the dome. In Fig. 15a it is illustrated how the spherical and elliptic membranes only transfer vertical actions on the basement, v_s and v_c respectively, while a no-tension profile requires that the base support can support a horizontal force h_n (Fig. 15b).

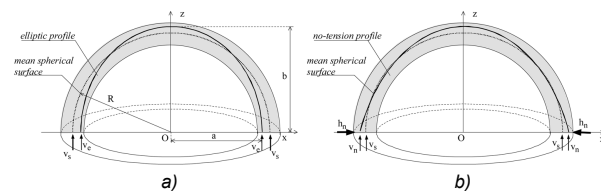


Fig. 15. No-thrust and no-tension stress surfaces: a) The basement of the dome is not subject to thrust action, but lower parallel lines are under tension; b) If a no-tension solution is adopted, the support of the dome is subject to a horizontal thrust force. Tension in the parallel lines is transferred to the basement

3.3. The effect of “masonry apparatus” on the statics of vaults. An help to intuition.

Reading masonry texture in a vault can help in understanding its equilibrium asset. The first element is indeed its geometry, a cross vault yields a equilibrium pattern different than a barrel vault, and so on. But a double-curvature surface, apart from its particular conception is anyway a highly hyperstatic system, and the equilibrium is never uniquely determinate. So the way the stones are jointed all together is a key to understand what equilibrium path would stresses run through, and/or what path would the builder have preferred to drive the vault to accommodate in.

So, consider for instance the two vaults in Fig. 16a and in Fig. 16b, having the same geometry, but in vault a) the mortar rows are parallel to the base perimeter, while in the vault b) the mortar rows are normal to the perimeter. The postulate is that compression normal to the mortar rows is the preferred equilibrium path for the vault, and that this is the tool for the original builder to steer the vault into a (his) objective static asset. If the preferred direction for compression is normal to the perimeter, it is expected that compression acts along the arrows drawn in Figs. 3.8, a) and b), so that the vault gains a tensile capacity in the direction orthogonal to the arrows. It is easy to understand that this produces an effect on the thrust the vault exerts on the base supports. Consider in fact that in both cases the vault is made by four gores. In the case a) compression is directly transferred to the sides of the basement, while lateral dilatation and the diffusion of stresses to the corners is contrasted by internal tensile strength; so two opposite gores tend to directly sustain each other, and the distribution of the horizontal thrust force tends to concentrate towards the middle of the sides (Fig. 16c). By contrast, in case b) compression is active in the direction parallel to the base sides, and the gores tend to support each other along the diagonal lines, while the orthogonal dilatation and diffusion of stress are now contrasted by tensile strength in the direction orthogonal to the sides; so all forces tend to converge in the corners, and the distribution of the horizontal thrust force tends to concentrate to the corners (Fig. 16d). In other words, by acting on the masonry apparatus it is possible that, with the same geometry, a structure may be realized that works like a cloister vault rather than like a groin vault or viceversa. Which means that it may be not wise to analyze the statics of a vault only on the basis of its geometry. Anyway, a skilled design of apparatus is also a tool to build vaults without formworks [13].

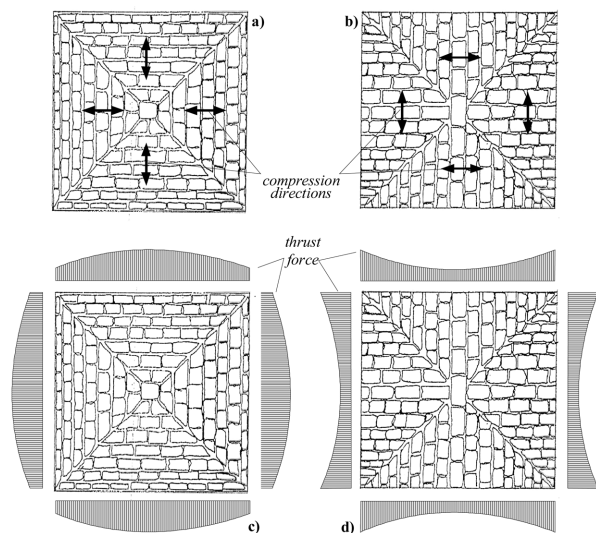


Fig. 16. Influence of the vault apparatus on the static behaviour of vaults. The difference in the apparatus in Figs. a) and b) yields a different equilibrium pattern and a different distribution of the thrust force as in Figs. c) and d)

4. MASONRY AS A NO-TENSION MATERIAL

In the previous section it has been recognized that in some cases a tensile capacity along some direction can be attributed to masonry. Anyway Eq. (1) is conditioned by the implicit as-

sumption that σ'_{ox} is not larger than σ'_{ob} , the tensile strength of single bricks. If in any time in the life of the structure the stress s exceeds this limit, the bricks crack, and the strength decays to zero, with a brittle behaviour. On the other side, there is no doubt that the prevalent feature that characterizes masonry structures, and makes them dissimilar from modern concrete and steel structures, is quite definitely their intrinsic inability to resist tensile stresses. So, it is natural that the material model, that is intended to be an “analogue” of real masonry, cannot resist tensile stress, but, possibly, behaves elastically under pure compression.

No-Tension solutions for masonry structures are however a very significant reference point and a powerful tool for reliable structural assessment, for many reasons. The first reason is that the NT model is a stable behaviour, poorly subject to uncertainty and aging. Tensile strength is in any case small, uncertain, highly variable in the mass of a structure, not durable in time and so on; anyway neglecting tensile strength leads to a safe assessment. In other words, no doubt that the NT model is a simplified behaviour, that in some cases does not give account of some surprisingly good performance of masonry buildings, but it is also true that if a masonry structure does not pass through a NT check it remains a suspect structure.

In the following the basics for the foundation of a NT material theory are illustrated, and the relevant principles for structural analysis, mainly identified in the classic energy theorems, suitably adapted to the material at hand, are formulated.

In (apparently) simple cases, closed-form solutions can be obtained, or, at least, the solution process can be prepared after a preliminary screening of the equilibrium scenario.

4.1. The standard No-Tension material

In a NT solid the equilibrium against external loads is required to be satisfied by *admissible* stress fields, which imply pure compression everywhere in the solid. Compatibility of the strain field can be ensured by superposing to the elastic strain field an additional *fracture* field, that does not admit contraction in any point and along any direction; that is to say that the stress tensor σ must be negative semi-definite everywhere in the solid, while the fracture strain field ϵ_f is required to be positive semi-definite.

The material shall, hence, satisfy the following conditions

$$\epsilon = \epsilon_e + \epsilon_f = C\sigma + \epsilon_f$$

$$\text{Semi-Definite} \begin{cases} \epsilon_f & \text{Positive} \\ \sigma & \text{Negative} \end{cases} \rightarrow \begin{cases} \epsilon_{fa} \geq 0 \\ \sigma_a \leq 0 \end{cases} \quad \forall a \in r_a \quad (17)$$

$$\sigma \cdot \epsilon_f \leq 0$$

where r_a is the set of directions through the generic point in the solid, a is one of such directions, ϵ_f is the fracture strain that is assumed to superpose to the elastic strain ϵ_e in order to anneal tensile stresses if possible, and C denotes the tensor of elastic constants. Consider moreover that on every elementary surface with normal a , if ϵ_{fa} is strictly positive σ_a must be zero; by contrast if σ_a is strictly negative, ϵ_{fa} must be zero. If σ_o is the stress tensor in the point actually associated with fractures ϵ_f , it follows that

$$\sigma_o \cdot \epsilon_f = 0 \quad (18)$$

The material admissibility conditions for strain and stress reported in Eq.(1) can be synthetically referred to by the set of inequalities $\mathbf{h}_\varepsilon(\boldsymbol{\varepsilon}_f) \geq \mathbf{0}$ and $\mathbf{h}_\sigma(\boldsymbol{\sigma}) \geq \mathbf{0}$ respectively.

As a consequence of Eqs. (17) and (18), the classical Drucker's rule holds for the fracture strain. With reference to the admissible domains quoted in Eq. (4.1), the normality Drucker's law for no-tension material can thus be written as

$$(\boldsymbol{\sigma} - \boldsymbol{\sigma}_o) \cdot \boldsymbol{\varepsilon}_f \leq 0 \quad \forall \boldsymbol{\sigma} \in \Sigma \quad (19)$$

where Σ is the set of admissible stress tensors and $\boldsymbol{\sigma}$ is any admissible stress state other than the effective one $\boldsymbol{\sigma}_o$.

4.2. Limit Analysis and fundamental theorems

Let consider the body and surface forces, \mathbf{F} acting on volume V and \mathbf{p} acting on the free surface S_p , the displacement field \mathbf{u} , the imposed displacement field \mathbf{u}_o characterizing the constrained part of the solid surface S_u , the above mentioned strain field $\boldsymbol{\varepsilon} = \boldsymbol{\varepsilon}_e + \boldsymbol{\varepsilon}_f = \mathbf{C} \boldsymbol{\sigma} + \boldsymbol{\varepsilon}_p$, the stress field $\boldsymbol{\sigma}$.

As clear from the above, fracture strains $\boldsymbol{\varepsilon}_f$ can be developed at the considered point only if the stress situation can be represented by a stress tensor $\boldsymbol{\sigma}$ laying on the surface of the material admissibility domain, which is defined for NT bodies by $\mathbf{h}_\sigma(\boldsymbol{\sigma}) \leq \mathbf{0}$; obviously if some fracture does exist, it is developed according to the NT material inequalities $\mathbf{h}_\varepsilon(\boldsymbol{\varepsilon}_f) \geq \mathbf{0}$.

4.2.1. General setup

Denoting by U the set of possible displacement fields, the class of *fracture admissible mechanisms* is defined by the subset U_f of U containing displacement fields \mathbf{u}_f that are directly compatible with fracture strains $\boldsymbol{\varepsilon}_f$ apart from any elastic strain field

$$\boldsymbol{\varepsilon}_f = \nabla \mathbf{u}_f ; \mathbf{h}_\varepsilon(\boldsymbol{\varepsilon}_f) \geq \mathbf{0} \quad (20)$$

$$U_f = \{ \mathbf{u}_f \in U : \mathbf{h}_\varepsilon(\nabla \mathbf{u}_f) \geq \mathbf{0} \} \quad (21)$$

Collapse mechanisms can be defined as fracture admissible mechanisms \mathbf{u}_f such that the mechanical work developed by the applied loads (\mathbf{p}, \mathbf{F}) is positive; this condition is analytically expressed by the inequality

$$\int_{S_p} \mathbf{p} \cdot \mathbf{u}_f dS + \int_V \mathbf{F} \cdot \mathbf{u}_f dV > 0 \quad (22)$$

By the Principle of Virtual Work, a necessary condition for the existence of any admissible stress field $\boldsymbol{\sigma}$ equilibrating the applied loads is that

$$\int_{S_p} \mathbf{p} \cdot \mathbf{u}_f dS + \int_V \mathbf{F} \cdot \mathbf{u}_f dV = \int_V \boldsymbol{\sigma} \cdot \boldsymbol{\varepsilon}_f dV \leq 0 \quad \forall \mathbf{u}_f \in U_f \quad (23)$$

After Eq. (23) one can enounce the "Kinematical Theorem" of Limit Analysis for NT bodies: *if any collapse mechanism exists under the applied loads, no solution can exist for the equilibrium of the NT solid*. In other words: *If any collapse mechanism exists, the solid collapses*.

On the other side, *statically admissible stress fields* $\boldsymbol{\sigma}$ can be defined as tensor fields equilibrating the applied loads and satisfying admissibility conditions, i.e. $\mathbf{h}_\sigma(\boldsymbol{\sigma}) \leq \mathbf{0}$ or $\boldsymbol{\sigma} \in \Sigma$, where

Σ is the admissible domain, everywhere in the solid. Assuming that under the load pattern (\mathbf{p}, \mathbf{F}) a statically admissible stress field $\boldsymbol{\sigma}$ exists for any mechanism \mathbf{u}_f , after Eq. (23) one gets

$$\int_{S_p} \mathbf{p} \cdot \mathbf{u}_f dS + \int_V \mathbf{F} \cdot \mathbf{u}_f dV \leq 0 \quad \forall \mathbf{u}_f \in U_f \quad (24)$$

One can, thus, enounce the "Static Theorem" of Limit Analysis for NT bodies: *if under the applied loads any statically admissible stress field $\boldsymbol{\sigma}$ exists, no collapse mechanism exists and the structure cannot collapse*.

4.2.2. The one-multiplier load pattern. The safety factor

Let assume the applied loads as given by the sum of a fixed component ($\mathbf{F}_o, \mathbf{p}_o$) and a variable component ($s\mathbf{F}_v, s\mathbf{p}_v$) depending on the value assumed by the multiplier s (actually one thus assumes that only the portion $\mathbf{F}_v, \mathbf{p}_v$, may be destabilizing and should be controlled)

$$\begin{cases} \mathbf{F} = \mathbf{F}_o + s\mathbf{F}_v = \mathbf{0} & \text{in } V \\ \mathbf{p} = \mathbf{p}_o + s\mathbf{p}_v & \text{on } S_p \end{cases} \quad (25)$$

and let define two fundamental classes of load multipliers s for NT bodies: the class of *statically admissible multipliers* β and the class of *kinematically sufficient multipliers* γ . After denoting by $\boldsymbol{\alpha}_n$ the unit outgoing vector normal to the surface S_p , load multipliers β are defined to be statically admissible if the following relations hold

$$\begin{cases} \text{div } \boldsymbol{\sigma}^\beta + \mathbf{F}_o + \beta\mathbf{F}_v = \mathbf{0} & \text{in } V \\ \boldsymbol{\sigma}^\beta \boldsymbol{\alpha}_n = \mathbf{p}_o + \beta\mathbf{p}_v & \text{on } S_p \end{cases} \quad (26)$$

$$\mathbf{h}_\sigma(\boldsymbol{\sigma}^\beta) \leq \mathbf{0} \quad (27)$$

that is to say, if a stress field $\boldsymbol{\sigma}^\beta$ exists equilibrating the applied loads with $s = \beta$ and satisfying the NT material admissibility conditions. A stress field satisfying Eqs (26) and (27) is qualified as *statically admissible*.

On the other side, load multipliers γ are defined to be *kinematically sufficient* if the following relations hold

$$\begin{cases} \boldsymbol{\varepsilon}_f^\gamma = \nabla \mathbf{u}_f^\gamma & \text{in } V \\ \mathbf{u}_f^\gamma = \mathbf{0} & \text{on } S_u \end{cases} \quad (28)$$

$$\mathbf{h}_\varepsilon(\boldsymbol{\varepsilon}_f^\gamma) \geq \mathbf{0} \quad (29)$$

$$\begin{aligned} & \int_V \mathbf{F}_o \cdot \mathbf{u}_f^\gamma dV + \int_{S_p} \mathbf{p}_o \cdot \mathbf{u}_f^\gamma dS + \\ & + \gamma \int_V \mathbf{F}_v \cdot \mathbf{u}_f^\gamma dV + \gamma \int_{S_p} \mathbf{p}_v \cdot \mathbf{u}_f^\gamma dS > 0 \end{aligned} \quad (30)$$

(with ∇ the symmetrical gradient operator), that is to say, if any displacement field \mathbf{u}_f^γ exists (a *collapse mechanism*) directly compatible with a NT admissible fracture strain $\boldsymbol{\varepsilon}_f^\gamma$ apart from any elastic strain field, and such that the condition stated by Eq.(30) is also satisfied. It is understood that the body is stable under the basic load pattern ($\mathbf{F}_o, \mathbf{p}_o$), and that Eq. (30) cannot be satisfied by any fracture strain field for $\gamma = 0$. In other terms it is assumed that the basic loads are suitably chosen in way that they cannot produce collapse.

Extensions to NT continua of the fundamental *static and kinematic theorems* of Limit Analysis allow individuating the value \bar{s} of the load multipliers s , limiting the loading capacity of the body.

On the basis of the *static theorem*, one can state that “the collapse multiplier \bar{s} represents the maximum of the statically admissible multipliers β ”

$$\bar{s} = \max\{\beta \in B_o\} \quad (31)$$

where B_o is the class of statically admissible multipliers.

On the basis of the *kinematic theorem*, one can state that “the collapse multiplier \bar{s} represents the minimum of the kinematically sufficient multipliers γ ”

$$\bar{s} = \min\{\gamma \in \Gamma_o\} \quad (32)$$

where Γ_o is the class of kinematically sufficient multipliers.

Thereafter, by means of the static theorem, one can search for the collapse multiplier by implementing the problem

$$\begin{aligned} & \text{Find: } \max\{\beta\} \\ & \quad \beta, \sigma^\beta \\ \text{Sub } & \begin{cases} \text{div } \sigma^\beta + \mathbf{F}_o + \beta \mathbf{F}_v = \mathbf{0} & \text{in } V \\ \sigma^\beta \boldsymbol{\alpha}_n = \mathbf{p}_o + \beta \mathbf{p}_v & \text{on } S_p \end{cases} \text{ and } \mathbf{h}_\sigma(\sigma^\beta) \leq \mathbf{0} \end{aligned} \quad (33)$$

Or otherwise, by means of the kinematic theorem, by solving the problem

$$\begin{aligned} & \text{Find: } \min\{\gamma\} \quad \text{Sub } \begin{cases} \boldsymbol{\varepsilon}_f^\gamma = \nabla \mathbf{u}_f^\gamma & \text{in } V \\ \mathbf{u}_f^\gamma = \mathbf{0} & \text{on } S_u \end{cases} \text{ and} \\ & \begin{cases} \mathbf{h}_\varepsilon(\boldsymbol{\varepsilon}_f^\gamma) \geq \mathbf{0} \\ \int_V \mathbf{F}_o \cdot \mathbf{u}_f^\gamma dV + \int_{S_p} \mathbf{p}_o \cdot \mathbf{u}_f^\gamma dS + \gamma \int_V \mathbf{F}_v \cdot \mathbf{u}_f^\gamma dV + \gamma \int_{S_p} \mathbf{p}_v \cdot \mathbf{u}_f^\gamma dS > 0 \end{cases} \end{aligned} \quad (34)$$

4.3. Variational principles for the NT equilibrium problem

Analysis of no-tension structures proves that stress, strain and displacement fields obey extremum principles of the basic energy functionals. Therefore the solution displacement and fracture strain fields are found as the constrained minimum of the *Potential Energy* functional, under the condition that the fracture field is positively semi-definite at any point. In other words, if $\boldsymbol{\varepsilon}$ and \mathbf{u} are respectively the strain and the displacement fields such that

$$\boldsymbol{\varepsilon} = \nabla \mathbf{u} \quad (35)$$

and \mathbf{p} , \mathbf{F} are the surface tractions and the body forces, it is possible to write down the Total Potential Energy (TPE) functional

$$\begin{aligned} \mathbf{E}(\mathbf{u}, \boldsymbol{\varepsilon}_f) &= \frac{1}{2} \int_V (\nabla \mathbf{u} - \boldsymbol{\varepsilon}_f) [\mathbf{D}(\nabla \mathbf{u} - \boldsymbol{\varepsilon}_f)] dV - \\ & - \int_{S_p} \mathbf{p} \cdot \mathbf{u} dS - \int_V \mathbf{F} \cdot \mathbf{u} dV = L(\mathbf{u}, \boldsymbol{\varepsilon}_f) + P(\mathbf{u}) \end{aligned} \quad (36)$$

with \mathbf{D} the inverse tensor of \mathbf{C} . The TPE functional $\mathbf{E}(\mathbf{u}, \boldsymbol{\varepsilon}_f)$ is made up by two terms, expressing the energy stored in the body $L(\mathbf{u}, \boldsymbol{\varepsilon}_f)$ and the opposite of the work made by the applied loads $P(\mathbf{u})$. It can be proved that the solution $\mathbf{u}_o, \boldsymbol{\varepsilon}_{f_o}$ satisfies the following condition

$$\mathbf{E}(\mathbf{u}_o, \boldsymbol{\varepsilon}_{f_o}) = \min_{\substack{\mathbf{u} \in U \\ \boldsymbol{\varepsilon}_f \in \Phi}} \mathbf{E}(\mathbf{u}, \boldsymbol{\varepsilon}_f) = \mathbf{E}_o \quad (37)$$

which is the minimum of the Potential Energy, conditioned upon admissibility of the fracture strain, with Φ the set of admissible fracture fields. Despite the quadratic functional $L(\mathbf{u}, \boldsymbol{\varepsilon}_f)$ is positive definite, the minimum may be not unique if some mechanism exists such that $P(\mathbf{u}) = 0$.

The stress field can be found, in turn, as the constrained minimum of the Complementary Energy (CE) functional, under the condition that the stress field is in equilibrium with the applied loads and compressive everywhere. In other words, let

$$\mathbf{S}(\boldsymbol{\sigma}) = \frac{1}{2} \int_V \boldsymbol{\sigma} \cdot \mathbf{C} \boldsymbol{\sigma} dV - \int_{S_u} \mathbf{T} \cdot \mathbf{u}_o dS = L_c(\boldsymbol{\sigma}) + R(\boldsymbol{\sigma}); \quad \mathbf{T} = \boldsymbol{\sigma} \boldsymbol{\alpha}_n \quad (38)$$

be the CE functional $S(\boldsymbol{\sigma})$ defined on the set Σ_o of the admissible stress fields ($\Sigma_o \subseteq \Sigma$) in equilibrium with the applied loads, with $L_c(\boldsymbol{\sigma})$ the complementary energy stored in the body and $R(\boldsymbol{\sigma})$ the work by the reactions times the settlements of the constrained points. It can be proved that, if $\boldsymbol{\sigma}_o$ is the solution stress field, the following condition holds

$$\mathbf{S}(\boldsymbol{\sigma}_o) = \min_{\boldsymbol{\sigma} \in \Sigma_o} \mathbf{S}(\boldsymbol{\sigma}) = \mathbf{S}_o \quad (39)$$

Eq.(39) expresses the compatibility condition on the solution stress field, i.e. the constrained minimum of $S(\boldsymbol{\sigma})$ yields the stress field $\boldsymbol{\sigma}_o$ such that the elastic strains $\mathbf{C} \boldsymbol{\sigma}_o$ can be made compatible with a continuous displacement field, by the superposition of a fracture strain field. Since $\boldsymbol{\sigma} \cdot \mathbf{C} \boldsymbol{\sigma}$ is positive definite in Σ , the solution is unique.

4.4. Convexity of the energy functionals and Limit Analysis as a tool for existence of the solution

It is easy to prove that the Total Potential Energy and the Complementary Energy functionals are both defined on convex sets. The respective sets of definition are: i) the space of couples $(\mathbf{u}, \boldsymbol{\varepsilon}_f)$, with \mathbf{u} a displacement vector function compatible with the external constraints and $\boldsymbol{\varepsilon}_f$ a semi-positively valued tensor field; ii) the space of semi-negatively valued tensor fields in equilibrium with the applied loads. Because of convexity, both minima exist if the respective definition sets, $U \times \Phi$ on one side and Σ_o on the other side, are not empty. For Σ_o to be not empty it is necessary and sufficient that the structure is under the collapse threshold; in this case a unique minimal point exists for $S(\boldsymbol{\sigma})$. U and Φ are intrinsically not empty, in that the first is the set of three-components vector fields and the second is the space of semi-positive definite 3rd-order tensor fields. The displacement/fracture solution may be not unique if a mechanism exists such that the external work is zero. Anyway, if any collapse mechanism exists, $E(\mathbf{u}, \boldsymbol{\varepsilon}_f)$ diverges, and the minimum does not exist.

It can be concluded that the solution of the NT equilibrium problem exists iff the structure is under the collapse threshold.

4.5. The NT solution for masonry arches and barrel vaults

NT solutions have been investigated since many years and many results have been produced, also yielding successful comparison with experimental results. As an example, consider the portal arch in Fig. 17a, that has been tested under an horizontal force acting on top of the right pillar, as in Fig. 17b. In Fig. 17c the comparison between the experimental and numerical results is plotted, proving a very good agreement of the NT theory with practice.

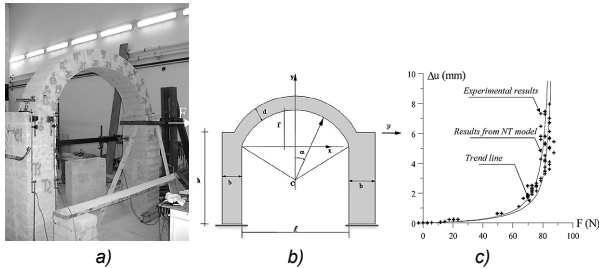


Fig. 17. Experimental and mechanical model: a) The laboratory arch-portal tested under the horizontal force F ; b) The mechanical NT model for calculations; c) Plot of numerical and experimental results

More details on NT material and structures can be found in [14, 15].

5. NO-TENSION MODEL FOR MASONRY – LIKE SHELLS AND DOMES

Equilibrium fields for No-Tension vaults can be built upon the assumption that a membrane stress-surface is considered, included in the profile of the vault, displaying compressive forces along all directions. The idea is not new, it was put forward by Heyman [11], but there are few doubts that it represents a powerful approach to search stresses in masonry vaults, as the 3D direct counterpart of the traditional historical method based on the funicular line of the loads in 2D structural problems (Fig. 18).

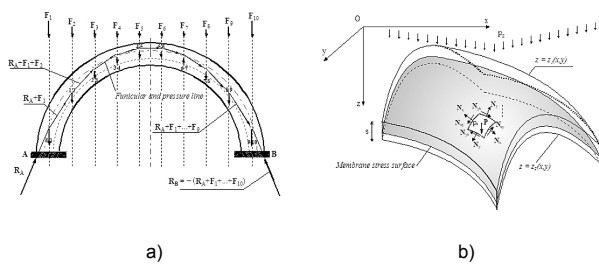


Fig. 18. a) Arch equilibrium analysis: the pressure line; b) Vault equilibrium analysis: the membrane stress surface

As illustrated in Sec. 4, modelling a large variety of equilibrium stress fields is the preliminary step to find a final solution, yielding a credible pattern for the fracture distribution, in agreement with technical expectation, as it can be recognized for the two-span arch in Fig. 19

In the following an approach is outlined to identify membrane stress surfaces both responding to the requirements of stress admissibility and equilibrium with active loads.

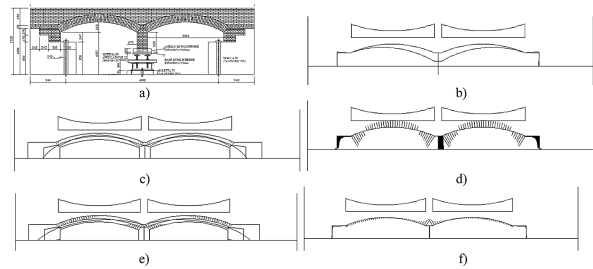


Fig. 19. Sample results from NT model. a) The arcade and the experimental set up; b) The arcade in the original configuration and with downward settlement of the central pier; c) Pressure line and fractures without settlement; d) Stresses without settlement; e) Pressure line and fractures with settlement; f) Stresses with settlement

5.1. Membrane 3D-equilibrium of the generic vault element

Let consider a membrane shell $z = z(x, y)$ subject to generic load components p_x, p_y, p_z , as shown in Fig. 20. In order to express local equilibrium conditions one should consider any single surface element under the action of loads and of membrane stresses, and write equilibrium equations along coordinate axes, as in Fig. 21.

After some algebra, the equilibrium equations in the x and y directions can be written in the form

$$\frac{\partial}{\partial x} \left(N_x \frac{\cos \varphi}{\cos \theta} \right) + \frac{\partial N_{xy}}{\partial y} = -p_x \frac{1}{\cos \varphi} \frac{1}{\cos \theta} \quad (40)$$

$$\frac{\partial N_{xy}}{\partial x} + \frac{\partial}{\partial y} \left(N_y \frac{\cos \theta}{\cos \varphi} \right) = -p_y \frac{1}{\cos \varphi} \frac{1}{\cos \theta} \quad (41)$$

Additionally, equilibrium along the z -direction yields

$$\left(\frac{\partial N_x}{\partial x} \frac{1}{\cos \theta} + \frac{\partial N_{xy}}{\partial y} \frac{1}{\cos \varphi} \right) \sin \varphi + \left(\frac{\partial N_{xy}}{\partial x} \frac{1}{\cos \theta} + \frac{\partial N_y}{\partial y} \frac{1}{\cos \varphi} \right) \sin \theta = -p_z \frac{1}{\cos \varphi} \frac{1}{\cos \theta} \quad (42)$$

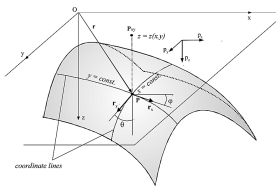


Fig. 20. The membrane surface

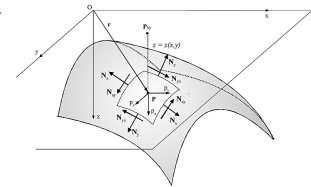


Fig. 21. Generic surface element of the membrane surface

5.2. Equivalence of the 3D-problem with the projected 2D-problem

Considering the projections $\bar{N}_x, \bar{N}_y, \bar{N}_{xy} = \bar{N}_{yx}$ of the membrane stresses onto the xy plane, as shown in Fig. 22

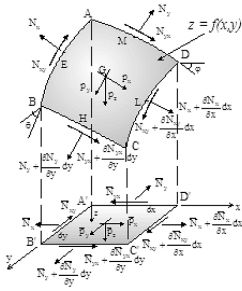


Fig. 22. Stresses and loads acting on a generic 3D-element of the vault mid-surface and their projection on the plane

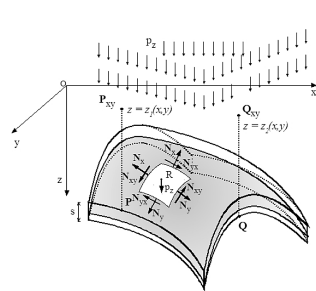


Fig. 23. The vault and its mid-surface under purely vertical loads

the following equations hold

$$\bar{N}_x = N_x \frac{\cos \varphi}{\cos \theta}, \quad \bar{N}_y = N_y \frac{\cos \theta}{\cos \varphi}, \quad \bar{N}_{xy} = N_{xy} \quad (43)$$

with

$$\tan \varphi = \frac{\partial z}{\partial x}, \quad \tan \theta = \frac{\partial z}{\partial y}. \quad (44)$$

Moreover putting

$$p_x = \bar{p}_x \cos \theta \cos \varphi, \quad p_y = \bar{p}_y \cos \theta \cos \varphi \quad (45)$$

the equilibrium equations in function of the new variables can be written

$$\frac{\partial \bar{N}_x}{\partial x} + \frac{\partial \bar{N}_{xy}}{\partial y} + \bar{p}_x = 0; \quad \frac{\partial \bar{N}_{xy}}{\partial x} + \frac{\partial \bar{N}_y}{\partial y} + \bar{p}_y = 0 \quad (46)$$

The z -equation, after some algebra, reduces to

$$\frac{\partial}{\partial x} \left(\bar{N}_x \frac{\partial z}{\partial x} + \bar{N}_{xy} \frac{\partial z}{\partial y} \right) + \frac{\partial}{\partial y} \left(\bar{N}_{xy} \frac{\partial z}{\partial x} + \bar{N}_y \frac{\partial z}{\partial y} \right) + \bar{p}_z = 0 \quad (47)$$

whence one gets

$$\bar{N}_x \frac{\partial^2 z}{\partial x^2} + 2\bar{N}_{xy} \frac{\partial^2 z}{\partial x \partial y} + \bar{N}_y \frac{\partial^2 z}{\partial y^2} = -\bar{p}_z + \bar{p}_x \frac{\partial z}{\partial x} + \bar{p}_y \frac{\partial z}{\partial y} \quad (48)$$

So the membrane equilibrium, apart from Eq. (48), becomes analogous to the problem of a plane panel.

5.3. Reduction of equilibrium conditions by means of the stress function

In most cases, it is advantageous to introduce a *stress function* $\Psi(x, y)$ that reduces the 3 equilibrium equations to one second-order equation as follows. By analogy with the panel problem, the equilibrium conditions in the x and y directions are identically satisfied if one puts

$$\bar{N}_x = \frac{\partial^2 \Psi}{\partial y^2} - \int \bar{p}_x dx, \quad \bar{N}_y = \frac{\partial^2 \Psi}{\partial x^2} - \int \bar{p}_y dy, \quad (49)$$

$$\bar{N}_{xy} = \bar{N}_{yx} = -\frac{\partial^2 \Psi}{\partial x \partial y}.$$

Then the third equilibrium equation (48) turns into

$$\frac{\partial^2 \Psi}{\partial x^2} \frac{\partial^2 z}{\partial y^2} - 2 \frac{\partial^2 \Psi}{\partial x \partial y} \frac{\partial^2 z}{\partial x \partial y} + \frac{\partial^2 \Psi}{\partial y^2} \frac{\partial^2 z}{\partial x^2} =$$

$$= -\bar{p}_z + \bar{p}_x \frac{\partial z}{\partial x} + \bar{p}_y \frac{\partial z}{\partial y} + \frac{\partial^2 z}{\partial x^2} \int \bar{p}_x dx + \frac{\partial^2 z}{\partial y^2} \int \bar{p}_y dy \quad (50)$$

The solution of the problem is, thus, reduced to the determination of the stress function. If $p_x = p_y = 0$ (e.g. the vault sustains only gravitational loads), the latter equation simplifies to:

$$\frac{\partial^2 \Psi}{\partial x^2} \frac{\partial^2 z}{\partial y^2} - 2 \frac{\partial^2 \Psi}{\partial x \partial y} \frac{\partial^2 z}{\partial x \partial y} + \frac{\partial^2 \Psi}{\partial y^2} \frac{\partial^2 z}{\partial x^2} = -\bar{p}_z \quad (51)$$

5.4. Stress NT admissibility

Let consider a masonry vault with thickness s , subject only to vertical loads, as shown in Fig. 23. Since it is assumed that the masonry cannot resist tensile stresses, the internal forces have to satisfy the following admissibility conditions

$$N_x \leq 0, \quad N_y \leq 0, \quad N_{xy}^2 - N_x N_y \leq 0 \quad (52)$$

A solution can be attempted searching for a membrane surface $z = z(x, y)$ completely internal to the mass of the vault, and such to resist the downward (i.e. positive) load p_z by purely compressive internal forces. The first condition is expressed by the inequalities (the *inclusion* condition)

$$z_1(x, y) \leq z(x, y) \leq z_2(x, y) \quad (53)$$

where $z_1(x, y)$ and $z_2(x, y)$ are the surfaces identifying the upper and lower profiles of the vault, respectively.

Definitively, setting the problem in plane variables and assuming that only vertical loads act, the equilibrium is expressed by Eqs. (49) with $p_x = p_y = 0$ and by Eq. (51), whilst admissibility conditions are given by

$$\left. \begin{array}{l} N_x \leq 0 \\ N_y \leq 0 \\ N_{xy}^2 - N_x N_y \leq 0 \end{array} \right\} \Leftrightarrow \left\{ \begin{array}{l} \bar{N}_x \leq 0 \\ \bar{N}_y \leq 0 \\ \bar{N}_{xy}^2 - \bar{N}_x \bar{N}_y \leq 0 \end{array} \right. \quad (54)$$

Eqs. (54) are conditioned by Eq. (53), according to which the stress membrane shell of the vault should be kept within the vault's profiles.

5.5. Simple coupling of stress equilibrium with admissibility

So, the key of the problem is how the stress function $\Psi(x, y)$ combines with the membrane function $z(x, y)$. It is interesting to note that if one takes

$$\Psi(x, y) = -k z(x, y), \quad k > 0 \quad (55)$$

by substitution in Eq.(49), one gets

$$\bar{N}_x = -k \frac{\partial^2 z}{\partial y^2}, \quad \bar{N}_y = -k \frac{\partial^2 z}{\partial x^2}, \quad \bar{N}_{xy} = \bar{N}_{yx} = k \frac{\partial^2 z}{\partial x \partial y}. \quad (56)$$

Coupling with admissibility conditions, one gets

$$\left. \begin{array}{l} \bar{N}_x \leq 0 \\ \bar{N}_y \leq 0 \\ \bar{N}_{xy}^2 - \bar{N}_x \bar{N}_y \leq 0 \end{array} \right\} \Leftrightarrow \left\{ \begin{array}{l} \frac{\partial^2 z}{\partial y^2} \geq 0 \\ \frac{\partial^2 z}{\partial x^2} \geq 0 \end{array} \right. \quad (57)$$

$$\left[\frac{\partial^2 z}{\partial x^2} \frac{\partial^2 z}{\partial y^2} - \left[\frac{\partial^2 z}{\partial x \partial y} \right]^2 \right] = \mathcal{H}_z(x, y) \geq 0$$

$$\forall (x, y) \in X$$

with $\mathcal{H}_z(x, y)$ the Hessian determinant of the z function, and X the horizontal projection of the vault. On the other side, substitution of Eq. (55) in the z -equilibrium Eq. (51) yields

$$\mathcal{H}_z(x, y) = \frac{\partial^2 z}{\partial x^2} \frac{\partial^2 z}{\partial y^2} - \left[\frac{\partial^2 z}{\partial x \partial y} \right]^2 = \frac{\bar{p}_z}{Q} \geq 0; \quad Q = 2k \quad (58)$$

with Q the thrust basement factor. From Eqs (57) one can deduce that $z(x, y)$ is a concave function. One can also observe that in a masonry vault, equilibrium may coincide with admissibility. This result means that a single joint equation is able to account at the meanwhile for both equilibrium and admissibility, also giving a scientific demonstration of the easiness of building masonry vaults, due to the almost immediate intuition of equilibrium against applied load, which is able to assure also admissibility.

Eq. (58) represents the simplest form of the well known Monge-Ampère equation [16], and quite clearly plays a key role in the statics of NT vaults [17].

5.6. General coupling of stress equilibrium with admissibility

More in general consider the position

$$\Psi(x, y) = F[z(x, y)] \quad (59)$$

Eq.s (49) turn to

$$\bar{N}_x = \frac{\partial^2 F}{\partial z^2} \left[\frac{\partial z}{\partial y} \right]^2 + \frac{\partial F}{\partial z} \frac{\partial^2 z}{\partial y^2}; \quad \bar{N}_y = \frac{\partial^2 F}{\partial z^2} \left[\frac{\partial z}{\partial x} \right]^2 + \frac{\partial F}{\partial z} \frac{\partial^2 z}{\partial x^2} \quad (60)$$

$$\bar{N}_{xy} = \bar{N}_{yx} = - \left(\frac{\partial^2 F}{\partial z^2} \frac{\partial z}{\partial y} \frac{\partial z}{\partial x} + \frac{\partial F}{\partial z} \frac{\partial^2 z}{\partial x \partial y} \right)$$

and Eqs. (54) yield

$$\left. \begin{array}{l} \bar{N}_x \leq 0 \\ \bar{N}_y \leq 0 \\ \bar{N}_{xy}^2 - \bar{N}_x \bar{N}_y \geq 0 \end{array} \right\} \Leftrightarrow \left\{ \begin{array}{l} \frac{\partial^2 F}{\partial z^2} \left[\frac{\partial z}{\partial y} \right]^2 + \frac{\partial F}{\partial z} \frac{\partial^2 z}{\partial y^2} \leq 0 \\ \frac{\partial^2 F}{\partial z^2} \left[\frac{\partial z}{\partial x} \right]^2 + \frac{\partial F}{\partial z} \frac{\partial^2 z}{\partial x^2} \leq 0 \end{array} \right. \quad (61)$$

$$\Leftrightarrow \left(\frac{\partial^2 F}{\partial z^2} \left[\frac{\partial z}{\partial y} \right]^2 + \frac{\partial F}{\partial z} \frac{\partial^2 z}{\partial y^2} \right) \left(\frac{\partial^2 F}{\partial z^2} \left[\frac{\partial z}{\partial x} \right]^2 + \frac{\partial F}{\partial z} \frac{\partial^2 z}{\partial x^2} \right) + \left[\frac{\partial^2 F}{\partial z^2} \frac{\partial z}{\partial y} \frac{\partial z}{\partial x} + \frac{\partial F}{\partial z} \frac{\partial^2 z}{\partial x \partial y} \right]^2 \leq 0$$

while the z -equilibrium Eq. (51) is

$$2 \frac{\partial F}{\partial z} \left(\frac{\partial^2 z}{\partial x^2} \frac{\partial^2 z}{\partial y^2} - \frac{\partial^2 z}{\partial x} \frac{\partial^2 z}{\partial y} \frac{\partial^2 z}{\partial x \partial y} \right) + \frac{\partial^2 F}{\partial z^2} \left[\left(\frac{\partial z}{\partial x} \right)^2 \frac{\partial^2 z}{\partial y^2} - 2 \frac{\partial z}{\partial y} \frac{\partial z}{\partial x} \frac{\partial^2 z}{\partial x \partial y} + \left(\frac{\partial z}{\partial y} \right)^2 \frac{\partial^2 z}{\partial x^2} \right] = -\bar{p}_z \quad (62)$$

5.7. Problem solution in terms of stress and fractures by the complementary energy approach

Once membrane forces have been identified, stresses and consequently elastic energy can be easily calculated.

Therefore, after individuating the set of statically admissible membrane surfaces (in terms of admissibility and equilibrium, i.e. satisfying the set of inequalities in Eqs (40)-(41)-(42) and (52)), a possible approach in order to find the solution in terms of stresses is to set up a Complementary Energy problem to be formulated as a kind of extension to masonry vaults of the classical analogous energetic approach for linearly elastic structures, aiming at finding the fracture field that yields a compatible strain field when combined with elastic strains.

In order to undertake this approach the expression of the Complementary Energy embedded in a masonry vault element shall be evaluated. In case of NT assumption, one should consider that the generic element appears to be partially resistant; with reference to Fig. 24 one has the following stress and strain components in the membrane's plane

$$\left\{ \begin{array}{l} \sigma_x(C_N) = \sigma_{mx} \left(1 + \frac{e_r}{d_{G_r}} \right) = \frac{N_x}{3u} \left(1 + \frac{e_r}{d_{G_r}} \right) \\ \sigma_y(C_N) = \sigma_{my} \left(1 + \frac{e_r}{d_{G_r}} \right) = \frac{N_y}{3u} \left(1 + \frac{e_r}{d_{G_r}} \right) \end{array} \right. \quad (63)$$

$$\left\{ \begin{array}{l} \varepsilon_x(C_N) = \frac{1}{E} [\sigma_x(C_N) - \nu \sigma_y(C_N)] \\ \varepsilon_y(C_N) = \frac{1}{E} [\sigma_y(C_N) - \nu \sigma_x(C_N)] \end{array} \right.$$

where C_N is the point where the membrane surface intersects the normal to the middle surface of the vault, u is the distance from C_N to the compressed profile of the vault element, the neutral surface where stresses are null is at distance $3u$ from the compressed profile, the part of the vault element below (or above) the neutral surface is inert and possibly fractured, $A_{rx} = 3uds_y$ and $A_{ry} = 3uds_x$ are the reactive areas of the respective cross-sections, G_r is the centroid of the reactive part of the vault element, e_r is the distance of the membrane from G_r , and N_x, N_y are the normal forces per unit length on the element edges; $\sigma_{mx} = \sigma_x(G_r)$, $\sigma_{my} = \sigma_y(G_r)$ are the average compression stresses on respectively A_{rx} and A_{ry}

$$\sigma_{mx} = \sigma_x(G_r) = \frac{N_x}{3u} \quad ; \quad \sigma_{my} = \sigma_y(G_r) = \frac{N_y}{3u} \quad (64)$$

Eqs. (63) and (64) after some algebra yield

$$\begin{cases} \sigma_x(C_N) = \frac{N_x}{3u} \left(1 + \frac{e_r}{d_{Gr}} \right) \\ \sigma_y(C_N) = \frac{N_y}{3u} \left(1 + \frac{e_r}{d_{Gr}} \right) \end{cases} \quad (65)$$

$$\begin{cases} \varepsilon_x(C_N) = \frac{1}{3uE} \left(1 + \frac{e_r}{d_{Gr}} \right) (N_x - \nu N_y) \\ \varepsilon_y(C_N) = \frac{1}{3uE} \left(1 + \frac{e_r}{d_{Gr}} \right) (N_y - \nu N_x) \end{cases}$$

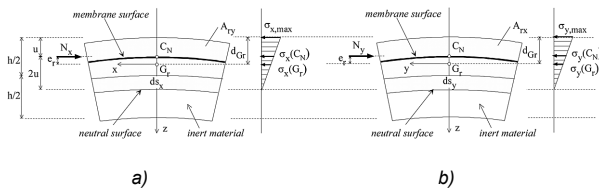


Fig. 24. Cross sections of the generic element of the vault and normal stresses distribution: a) Cross-section xz , b) Cross-section yz

When neglecting the curvatures of the element and the shear stress component, the elementary elastic work is

$$\begin{aligned} dL_e &= \frac{1}{2} [N_x \varepsilon_x(C_N) + N_y \varepsilon_y(C_N)] ds_x ds_y = \\ &= \frac{1}{6uE} \left(1 + \frac{e_r}{d_{Gr}} \right) (N_x^2 - 2\nu N_x N_y + N_y^2) ds_x ds_y \end{aligned} \quad (66)$$

and so is the elastic energy stored in the element $dL = dL_e$. The elastic energy over the whole vault is

$$\begin{aligned} L_e &= L = \int_S dL = \\ &= \frac{1}{6E} \int_S \frac{1}{3uE} \left(1 + \frac{e_r}{d_{Gr}} \right) (N_x^2 - 2\nu N_x N_y + N_y^2) ds_x ds_y \end{aligned} \quad (67)$$

where S is the mean surface of the vault. In Eq. (67) all the entities in the integrand function are dependent by the point coordinates through the membrane function $z(x,y)$.

The final Complementary Energy functional S expression is given by adding to the elastic energy term L , the energy related to the work developed by the constraint reactions R , as $S = L + R$.

The solution in terms of stresses shall be then searched for by numerically implementing the minimization of the Complementary Energy functional over admissible z -functions, i.e. under the condition that the solution itself is respectful of the above individuated equilibrium and admissibility equations.

6. SOLUTION OF NT EQUILIBRIUM. THE VAULTS OF TRANSLATION

After membrane forces have been identified, stresses and consequently elastic energy are easily calculated.

As shown in the previous paragraph, a possible approach to the problem consists in hypothesizing a shape of the stress

function $\Psi(x,y)$ a priori satisfying equilibrium and material admissibility, and, thereafter, deducing the related membrane function $z(x,y)$, and, therefore, stress distribution; in some cases this approach allows to identify solutions fitting some vault typologies; in the following, the case is presented of vaults of translation, such as the simple case of the barrel vault with indefinite length and the -less simple- barrel vault with constraints at its longitudinal extremities, which requires a rather more complex treatment.

6.1. The indefinite length barrel vault

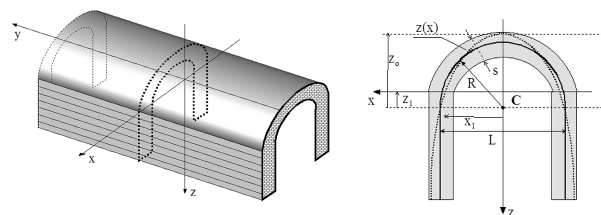


Fig. 25. The indefinite barrel vault and its cross-section

With reference to Fig. 25, consider the stress function in the form

$$\Psi(x, y) = -kz(x, y) + f(y) + g(x) \quad (68)$$

whence

$$\begin{aligned} \frac{\partial^2 \Psi(x, y)}{\partial x^2} &= -k \frac{\partial^2 z(x, y)}{\partial x^2} + g''(x); \quad \frac{\partial^2 \Psi(x, y)}{\partial y^2} = \\ &= -k \frac{\partial^2 z(x, y)}{\partial y^2} + f''(y); \quad \frac{\partial^2 \Psi(x, y)}{\partial x \partial y} = -k \frac{\partial^2 z(x, y)}{\partial x \partial y} \end{aligned} \quad (69)$$

From Eq.(51), equilibrium turns into

$$\begin{aligned} -2k \frac{\partial^2 z(x, y)}{\partial x^2} \frac{\partial^2 z(x, y)}{\partial y^2} + 2k \left(\frac{\partial^2 z(x, y)}{\partial x \partial y} \right)^2 + \\ + f''(y) \frac{\partial^2 z(x, y)}{\partial x^2} + g''(x) \frac{\partial^2 z(x, y)}{\partial y^2} = -\bar{p}_z(x, y) \end{aligned} \quad (70)$$

If one considers

$$\bar{p}_z(x, y) = \bar{p}_z(x); \quad z(x, y) = z(x) \quad (71)$$

Eq. (70) reduces to

$$f''(y) \frac{\partial^2 z(x)}{\partial x^2} = -\bar{p}_z(x) \quad (72)$$

which can be solved with

$$f''(y) = \text{const.} = -H; \quad H \geq 0 \quad (73)$$

whence

$$z''(x) = \frac{\bar{p}_z(x)}{H} \geq 0$$

$$\bar{N}_x = \frac{\partial^2 \Psi(x, y)}{\partial y^2} = f''(y) = -H \leq 0, \quad \bar{N}_y = \frac{\partial^2 \Psi(x, y)}{\partial x^2} =$$

$$= -kz''(x) + g''(x), \quad \bar{N}_{xy} = \frac{\partial^2 \Psi(x, y)}{\partial x \partial y} = 0$$

According to Eq. (56) the solution is admissible if $-kz''(x) + g''(x) \leq 0$. If one takes $-kz''(x) + g''(x) = 0$ the previous Eqs (73) yield $N_y = 0$, and the equation

$$z''(x) = \frac{\bar{p}_z(x)}{H} \geq 0 \quad (75)$$

yields the funicular line of the active load, with H the relevant thrust, which is the well known solution for the barrel vault as a sequence of independent arches (Fig. 25).

6.2. The confined barrel vault

A second case can be obtained setting

$$\Psi(x, y) = ay^2\alpha(x) \quad ; \quad z(x, y) = \frac{\Psi_0(x, y) - \Psi(x, y)}{2k} \quad (76)$$

with the coefficient a such that $0 \leq aL \leq 1$, being L a length parameter, and $\alpha(x)$ obeying the equation

$$q\alpha(x)\alpha''(x) - \alpha'^2(x) = k\bar{p}_z(x) \geq 0 \quad ; \quad q = 1/2 \quad (77)$$

One should notice that $\alpha(x)$ is the function governing the internal forces in the membrane surface. In fact, from Eq.(49), one has

$$\bar{N}_x(x, y) = \frac{\partial^2 \Psi(x, y)}{\partial y^2} = 2a\alpha(x); \quad \bar{N}_{xy}(x, y) = \frac{\partial^2 \Psi(x, y)}{\partial x \partial y} = 2ay\alpha'(x);$$

$$\bar{N}_y(x, y) = \frac{\partial^2 \Psi(x, y)}{\partial x^2} = ay^2\alpha''(x) \quad (78)$$

$\Psi_0(x, y)$ is assigned in the form

$$\Psi_0(x, y) = G(x)y^2 + Q(x) \quad (79)$$

with $G(x)$ and $Q(x)$ obeying the following differential equations

$$2a\alpha''(x)G(x) - 8a\alpha'(x)G'(x) + 2a\alpha(x)G''(x)y^2 = 8ka^2\bar{p}_z(x) \quad (80)$$

$$2a\alpha(x)Q''(x) = -2k\bar{p}_z(x)$$

The membrane surface remains identified by the equation:

$$z(x, y) = \frac{\Psi_0(x, y) - \Psi(x, y)}{2k} = \frac{G(x)y^2 + Q(x) - ay^2\alpha(x)}{2k} \quad (81)$$

The initial values of $\alpha(x)$, $G(x)$, $Q(x)$ with the relevant derivatives, and the values of a and k remain undetermined and available to set additional constraints.

In fact, if the problem is symmetric in both directions $\langle x \rangle$ and $\langle y \rangle$, the following conditions shall be added:

$$\left(\frac{\partial z}{\partial x}\right)_{x=-\ell/2} = z_x\left(-\frac{\ell}{2}, y\right) =$$

$$= \frac{G'(-\ell/2)y^2 + Q'(-\ell/2) - ay^2\alpha'(-\ell/2)}{2k} = z_1(y) \leq 0 \quad (82)$$

$$\left(\frac{\partial z}{\partial x}\right)_{x=+\ell/2} = z_x\left(+\frac{\ell}{2}, y\right) =$$

$$= \frac{G'(+\ell/2)y^2 + Q'(+\ell/2) - ay^2\alpha'(+\ell/2)}{2k} = z_2(y) \geq 0$$

$$z_2(y) = -z_1(y) \quad \forall y \Rightarrow$$

$$\Rightarrow \begin{cases} G'(+\ell/2) + G'(-\ell/2) = a[\alpha'(+\ell/2) + \alpha'(-\ell/2)] \\ Q'(+\ell/2) = -Q'(-\ell/2) \end{cases} \quad (83)$$

still because of symmetry

$$\left(\frac{\partial z}{\partial x}\right)_{x=-\ell/2} = z_x\left(-\frac{\ell}{2}, y\right) =$$

$$= \frac{G'(-\ell/2)y^2 + Q'(-\ell/2) - ay^2\alpha'(-\ell/2)}{2k} = z_1(y) \leq 0$$

$$\left(\frac{\partial z}{\partial x}\right)_{x=+\ell/2} = z_x\left(+\frac{\ell}{2}, y\right) =$$

$$= \frac{G'(+\ell/2)y^2 + Q'(+\ell/2) - ay^2\alpha'(+\ell/2)}{2k} = z_2(y) \geq 0 \quad (84)$$

$$z_2(y) = -z_1(y) \quad \forall y \Rightarrow$$

$$\Rightarrow \begin{cases} G'(+\ell/2) + G'(-\ell/2) = a[\alpha'(+\ell/2) + \alpha'(-\ell/2)] \\ Q'(+\ell/2) = -Q'(-\ell/2) \end{cases}$$

Initial conditions for $\alpha(x)$, $G(x)$ and $Q(x)$ and the parameters a and k can be sought in order to meet the requirement that the membrane surface $z = z(x, y)$ is in the interior of the vault thickness everywhere. Note that the set functions satisfy the equations

$$\frac{\partial^2 \Psi}{\partial x^2} \frac{\partial^2 z}{\partial y^2} - 2 \frac{\partial^2 \Psi}{\partial x \partial y} \frac{\partial^2 z}{\partial x \partial y} + \frac{\partial^2 \Psi}{\partial y^2} \frac{\partial^2 z}{\partial x^2} = -\bar{p}_z(x) \quad (85)$$

$$\frac{\partial^2 \Psi}{\partial x^2} \frac{\partial^2 \Psi}{\partial y^2} - \left(\frac{\partial^2 \Psi}{\partial x \partial y}\right)^2 = \rho(y)k\bar{p}_z(x) > 0$$

$$\frac{\partial^2 \Psi}{\partial x^2} \frac{\partial^2 \Psi_0}{\partial y^2} - 2 \frac{\partial^2 \Psi}{\partial x \partial y} \frac{\partial^2 \Psi_0}{\partial x \partial y} + \frac{\partial^2 \Psi}{\partial y^2} \frac{\partial^2 \Psi_0}{\partial x^2} =$$

$$= -[1 - \rho(y)]2k\bar{p}_z(x) \quad (86)$$

with $0 \leq \rho(y) \leq 1$ for any y , i.e. equilibrium and admissibility vs. vertical load are verified.

If one looks at the z -surface resulting from the above positions, one realizes that this can be assumed as the membrane surface for a confined barrel vault (Fig. 26).

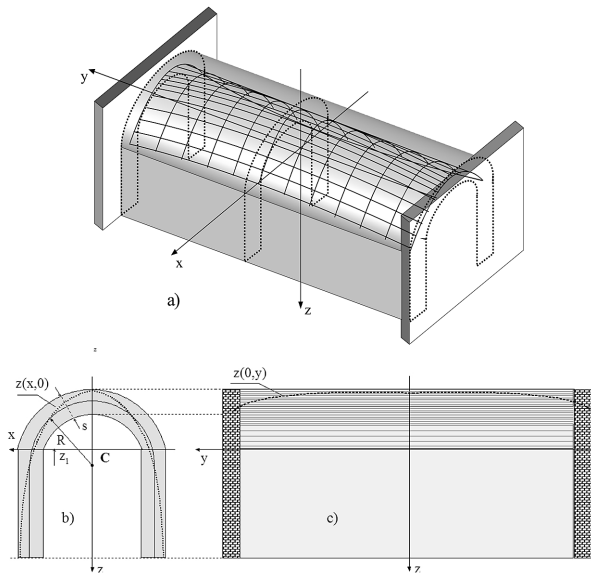


Fig. 26. The confined barrel vault with a possible membrane surface: a) Axonometric projection; b) Transverse xz section; c) Longitudinal yz section

7. VAULTS OF GENERAL SHAPE. THE MONGE-AMPERE EQUATION

The set S of solutions of the *Vault Inequality System (VIS)* composed by the inequalities

$$\begin{cases} \mathcal{H}_z(x, y) = z_{,xx}z_{,yy} - (z_{,xy})^2 \geq 0 \\ z_{,xx}(x, y) \geq 0 ; z_{,yy}(x, y) \geq 0 \quad \forall (x, y) \in X \\ z_1(x, y) \leq z(x, y) \leq z_2(x, y) \end{cases} \quad (87)$$

with X the horizontal projection of the vault, contains all solutions of the z -equilibrium Eq. (58). Solutions of the system Eq. (87) define convex functions $z(x, y)$ included in the profile of the vault, and enjoy the following property: If $z_i(x, y)$ ($i = 1, \dots, N$) are N functions, each verifying the, possibly homogeneous, basic VIS system in Eq. (87), any convex combination of such functions also yields a member of the solution set of the vault inequality with the strict inequality sign. The homogeneous VIS is the same as Eq. (87) with the sign of equality in the first row.

7.1. Finding solutions

It is possible to build up a number N of solutions $z_i(x, y)$ ($i = 1, \dots, N$) of the homogeneous or non-homogeneous VIS, so that solutions of the z -equilibrium equation

$$Q \cdot \mathcal{H}_z(x, y) - p_z(x, y) = 0 \quad (88)$$

can be searched in the form

$$z(x, y|c_i) = \sum_{i=1}^M c_i z_i(x, y) \quad (89)$$

where each of the basic functions $z_i(x, y)$ is assumed to comply with the VIS [Eq. (87)], in homogeneous or non-homogeneous form.

Assume, moreover, that some c_{oi} coefficients have been found such that

$$z_o(x, y|c_i) = \sum_{i=1}^M c_{oi} z_i(x, y) \quad (90)$$

verifies the inclusion condition. To this aim, it is sufficient that Eq. (90) is a convex combination of the basic z_i 's, possibly approaching as much as possible the middle surface $z_m(x, y)$.

Coefficients c_i yielding solutions of Eq. (88) correspond to the minimum of the error function

$$\begin{aligned} \mathcal{E}_0(c_i, Q) &= \int_X [Q \mathcal{H}_z(x, y|c_i) - \bar{p}_z(x, y)]^2 dx dy = \\ &= Q^2 S(c_i) - 2QR(c_i) + V \end{aligned} \quad (91)$$

with

$$\begin{aligned} S(c_i) &= \int_X [\mathcal{H}_z(x, y|c_i)]^2 dx dy \geq 0 \\ R(c_i) &= \int_X [\mathcal{H}_z(x, y|c_i) \bar{p}_z(x, y)] dx dy \\ V &= \int_X [\bar{p}_z(x, y)]^2 dx dy > 0 \end{aligned} \quad (92)$$

One should notice that, since $z(x, y|c_i)$ is assumed to be convex, also $R(c_i) \geq 0$ and because of the Schwarz's inequality

$$S(c_i)V - R^2(c_i) \geq 0 \quad (93)$$

The conditions for the minimum of Eq. (91) with respect to Q are written

$$\begin{aligned} \left. \frac{\partial \mathcal{E}_0(c_i, Q)}{\partial Q} \right|_{Q=Q^*} &= 2Q^* S(c_i) - 2R(c_i) = 0 \\ \left. \frac{\partial^2 \mathcal{E}_0(c_i, Q)}{\partial Q^2} \right|_{Q=Q^*} &= 2S(c_i) \geq 0 \end{aligned} \quad (94)$$

whence

$$Q^* = \frac{R(c_i)}{S(c_i)} = \frac{\int_X [\mathcal{H}_z(x, y|c_i) \bar{p}_z(x, y)] dx dy}{\int_X [\mathcal{H}_z(x, y|c_i)]^2 dx dy} \geq 0 \quad (95)$$

After substitution in the expression in Eq. (91) of the mean square error, one gets

$$\begin{aligned} \mathcal{E}^*(c_i) &= \mathcal{E}_0(c_i, Q^*) = Q^{*2} S(c_i) - 2Q^* R(c_i) + V = \\ &= V - \frac{R^2(c_i)}{S(c_i)} = \frac{1}{S(c_i)} [S(c_i)V - R^2(c_i)] \end{aligned} \quad (96)$$

By virtue of Eqs. (92)-(93), $\mathcal{E}^*(c_i)$ is a positive definite function of its arguments c_i and it is null if $\mathcal{H}_z(x, y) = \bar{p}_z(x, y)$.

It follows that the minimum of $\mathcal{E}^*(c_i)$ is attained where the ratio $\sim R^2(c_i)/S(c_i)$ is minimum. Therefore the problem can be definitely set in the form

$$\begin{aligned} \mathcal{E}(c_i) &= -\frac{R^2(c_i)}{S(c_i)} \\ \mathcal{E}(c_i^*) &= \mathcal{E}^* = \min_{c_i} -\frac{R^2(c_i)}{S(c_i)} \\ z_1(x, y) &\leq z(x, y|c_i) \leq z_2(x, y) \quad \forall (x, y) \in X \end{aligned} \quad (97)$$

All load patterns $\bar{p}_z(x, y)$ such that coefficients c_i resulting in $\mathcal{E}^* = 0$ exist, are called *manageable load patterns* with respect to the assumed form for the function $z(x, y|c_i)$. If the applied load is manageable, equilibrium can be exactly satisfied. Otherwise, equilibrium can be approximately verified, to some extent, depending on the choice of the basic functions $z_i(x, y)$.

Further details and applications are illustrated in [17, 18]. Interaction with the reciprocal problem, i.e. No-Compression double curvature structures, can give fruitful contributes to new developments (see e.g. [19]).

7.2. Some results. The NT vault subject to the self-weight and to a manageable live load

As an example, a parabolic vault covering a rectangular domain $X = [x_1, x_2] \times [y_1, y_2]$. The vault is characterized by height f , thickness s and middle surface

$$\bar{z}_m(x, y) = a(x^2 + y^2) + s \quad (98)$$

with $a = f/(x_1^2 + y_1^2)$.

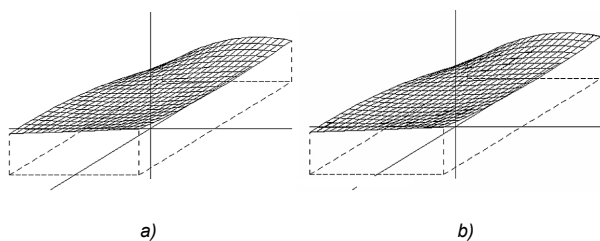


Fig. 27. Sample results: a) Plot of the objective load $p(x, y) = w(x, y) + q(x, y)$; b) Superposition of the objective load and its approximation by means of $\mathcal{H}_z(x, y)$; the two plots are practically coincident

The objective load is composed by the superposition of an accidental load $q(x, y)$ localized around a point (x_0, y_0) and the self weight of the vault $w(x, y)$ given as follows

$$w(x, y) = \gamma_f [\bar{z}_1(x, y) + t] + \gamma_m s \quad (99)$$

with t denoting the height of the superstructure, γ_f and γ_m the unit weight of the superstructure and of the structural masonry respectively.

A manageable live load is assumed in the form

$$q(x, y) = q_0 \left[(x_1 - x_0)^2 (y_1 - y_0)^2 - (x - x_0)^2 (y - y_0)^2 \right] \quad (100)$$

and the results are plotted in Fig. 27, proving a perfect agreement between the Hessian $\mathcal{H}_z(x, y)$ of the function $z(x, y)$ and the objective load $p(x, y) = w(x, y) + q(x, y)$.

A second example is quoted in Fig. 28, where a live load, non-manageable with respect to the basis adopted for $z(x, y)$ is assumed in the form

$$q(x, y) = q_0 \exp \left\{ - \left[\frac{(x - x_0)^2}{2\Delta_x^2} + \frac{(y - y_0)^2}{2\Delta_y^2} \right] \right\} \quad (101)$$

The results are not coincident, but anyway a good approximation can be obtained. Better results can be pursued, of course, assuming an expression for $z(x, y)$ that makes the load manageable. Results are synthetically quoted in Fig. 28.

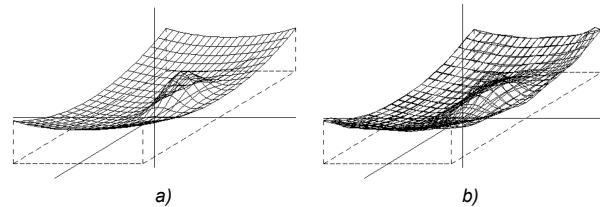


Fig. 28. Non-manageable load pattern: a) Plot of the objective load $p(x, y) = w(x, y) + q(x, y)$; b) Superposition of the objective load and its approximation by means of $\mathcal{H}_z(x, y)$

8. CONCLUSIONS

Historical masonry vaults and/or cupolas exhibit a large variety of typological assets. Often masonry is well operated, with strong stones and effectively adhesive mortar; in many cases masonry is in worse working order; in other cases a poor masonry is encountered.

Anyway, double-curvature structures can appeal to many equilibrium patterns to sustain at least their own weight plus some light additional loads. So they are in general stable systems, provided that their supports are strong and able to contrast thrust forces. Vaults are in general characterized by their shape, and a lot of types can be listed (see e.g. [20]), that have been conceived to be included in any simple or complex architectural design. But the equilibrium paths are also driven by the way masonry is interwoven. In some cases, a masterly design of the masonry tissue and of the vault apparatus may help in improving the structure's stability, and sometimes even in preventing fractures, as discussed and illustrated in Sec. 3.

It should be realized, by contrast, that fractures are almost always a physiological feature of masonry; since almost always it does not enjoy significant tensile strength, it cannot expand by tension and, when necessary to comply with congruence of the overall deformation, dilatation is provided by fractures.

Anyway, the poor consistency of the tensile resistance of the masonry material, its brittle, desultory and time-aging character, the difficulty in identifying non-zero reliable values, possibly led the ancient builders to introject empirical rules aiming, more or less consciously, at organizing structures in way that they are able to equilibrate loads without needing tensile stresses in the material. A susceptibility that has not been disproved by any analysis performed by modern powerful theoretical, numerical and electronic equipments. After a similar survey, Heyman, in 1966 [21], demonstrated that the failure of the masonry structures was substantially due to the activation of a collapse mechanism, rather than to the probability of compression crushing.

Many efforts have been devoted to specializing the Limit Analysis theory to the case of masonry structures (see e.g. [22-27]). Actually by referring to the collapse condition, one can just obtain some indications about the safety margins, whilst nothing about the fracture distribution or the behaviour evolution with increasing loads can be predicted.

Under such perspective, even if the NT model still represents an idealization of the real behaviour, one can follow the fracture evolution, assuming the small localized fractures as a phenomenological feature of the masonry material, besides the cases when the crack situation is such to compromise the local material resistance or to activate a collapse mechanism. The special character of the model, which results in an overall non-linear behaviour due to the unilateral nature of the constitutive law, and in a few more features related to the basic assumptions (determining and governing the existence of the inelastic crack strain field, the conditions for its activation, its development at the first detachment, the characteristics of the stress state), require some special formulation for structural analysis purposes (Sec.4).

Definitely, the solution of the structural problem is based on a suitable re-formulation of the energetic theorems, which, by reflecting the non-linear character of the mechanical model, translates into constrained extremum principles the ordinary conditions of stress equilibrium on one side, and of strain congruence on the other side. In such a way, the final state of the structural solid under different load levels can be identified up to the collapse situation, which can be predicted, as mentioned in the above, by means of the fundamental theorems of Limit Analysis, suitably re-formulated. As far as two-dimensional structural systems are concerned (walls, arches, plane models of masonry bridges and so on), and some their combinations, theory and practice are in a well established state of the art.

Application to the statics of vaults and cupolas is today largely investigated by many authors. The present paper is far from aiming at an exhaustive review, and only a few papers (see e.g. [28-33]) are referenced here, among the manifold that would deserve to be mentioned. It is clear however that

the problem is much harder than for plane structures; in this regard it may be enough to consider the intrinsic difficulties to identify collapse mechanisms in applying the kinematic approach of Limit Analysis to double-curvature vaults.

A common feature, however, is that in most cases the main objective is to extend to double-curvature roofing the methods that have historically developed with reference to single curvature arches or analogues, to find admissible stress distributions. The approach illustrated in Secs. 5-7, originally elaborated by the writers, aims at this purpose, on one side providing solution to the collapse problem from the point of view of the static theorem, and on the other side solving the preliminary step to find solutions including compatible strain and fracture fields in agreement with field engineering surveys. The Monge-Ampere equation, introduced in Sec. 5, is essentially the double-curvature counterpart of the equation of the funicular line. The equation has widely been investigated by mathematicians; nevertheless only a few solutions are available in the literature, so that solutions effective for the problem at hand shall be sought by specific and/or numerical methods. A Ritz-Galerkin type approach, requiring a previous identification of a number of basic functions, has been specifically issued in Sec. 7, proving its manageability in practical examples.

ACKNOWLEDGEMENT

The present research has been developed thanks to the financial support by the Dept. of "Protezione Civile" of the Italian Government, through the RELUIS Pool (Convention n. 823 signed 24/09/2009, Research Line n. AT2: 3), and to funds by MIUR (Italian Ministry for Education, University and Research) within a PRIN project.

REFERENCES

- [1] Baratta A. (2008) Gaudí: La forma della struttura. Fondamenti scientifici e tecnici di un processo progettuale e costruttivo (Italian). In Pane G. (ed): *Attualità di Antoni Gaudí. Teoria e prassi di un nuovo linguaggio architettonico*, Napoli, CLEAN, 48-55.
- [2] Benvenuto E. (1991) *An introduction to the history of structural mechanics. Part I, statics and resistance of solids. Part II, vaulted structures and elastic systems*. Springer-Verlag, New York.
- [3] Cowan H.J. (1977) A history of masonry and concrete domes in building construction. *Building and Environment*, 12, Pergamon Press, 1-24.
- [4] Huerta S. (2001) Mechanics of masonry vaults: In Lourenço P.B., Roca P. (eds.): *The equilibrium approach in Historical Constructions*. Guimarães, 47-69.
- [5] Huerta S. (2008) The analysis of masonry architecture: A historical approach. *Architectural Science Review*, 51(4), 297-328.
- [6] Hegemier G.A., Nunn R.O., Arya S.K. (1978) Behaviour of concrete masonry under biaxial stresses In: *Proc. North American Masonry Conf.*, University of Colorado, Boulder, U.S.A., paper 1.
- [7] Page A.W. (1981) The biaxial compressive strength of brick masonry. *Proc. Instn. of Civ. Engrs*, Part 2, 71, 893-906.
- [8] Baratta A. (2007) Apparecchio murario e statica delle strutture in muratura (Italian). *Notiziario dell' Ordine degli Ingegneri della Provincia di Napoli*, 2, 24-33.
- [9] Lenza P. (1983) Modelli di comportamento e direttrici di restauro delle scale in muratura realizzate con voltine a sbalzo (Italian). In: *Proceedings of the Workshop at the Faculty of Engineering of the University of Naples*, Istituto di Tecnica delle Costruzioni.
- [10] Baratta A., Corbi I. (2009) On masonry vaulted stairs: Statics and FRP reinforcement. In Di Tommaso A. (ed): *Proc. of the 3rd Nat. Conference on Mechanics of masonry structures reinforced by composites: modelling, experimentation, design and control (MuRiCo3)*, Venezia, 51-58.
- [11] Heyman, J. (1977) *Equilibrium of shell structures*, Oxford University Press, Oxford, pp. 134.
- [12] Farshad M. (1977) On the shape of momentless tensionless masonry domes. *Building and Environment*, 12(2), 81-85.
- [13] Wendland, D. (2005) Vaults built without formwork. In: *Proc. Int. Conf. on Theory and practice of construction: knowledge means, model-didactic and research experience*, Ravenna, Italy, 381-388.
- [14] Baratta A., Corbi O. (2010) An Approach to Masonry Structural Analysis by the No-Tension Assumption – Part

- I: Material Modeling, Theoretical Setup, and Closed Form Solutions. *Applied Mechanics Reviews*, 63(4), pp. 17.
- [15] Baratta A., Corbi O. (2010) An Approach to Masonry Structural Analysis by the No-Tension Assumption – Part II: Load Singularities, Numerical Implementation and Applications. *Applied Mechanics Reviews*, 63(4), pp. 21.
- [16] Gilbarg D., Trudinger N. S. (2001) *Elliptic Partial Differential Equations of Second Order*. Springer-Verlag, Berlin, 2nd Edition, pp. 544.
- [17] Baratta A., Corbi O. (2011) On the statics of No-Tension masonry-like vaults and shells: solution domains, operative treatment and numerical validation. *Annals of Solid and Structural Mechanics*, 2 (2-4), 107-122.
- [18] Baratta A., Corbi, O. (2010) On the Equilibrium and Admissibility Coupling in NRT Vaults of General Shape. *International Journal of Solids and Structures*, 47(17), 2276-2284.
- [19] Zhang J.Y., Ohsaki M. (2006) Adaptive force density method for form-finding problem of tensegrity structures. *International Journal of Solids and Structures*, 43, 5658-5673.
- [20] Donghi D. (1906) *Manuale dell' Architetto* (Italian), Vol. I, Part I. Ed. UTET, Torino
- [21] Heyman, J. (1966) The stone skeleton. *Journal of Solids and Structures*, 2, 269-279.
- [22] Orduña A., Lourenço P.B. (2001) Limit analysis as a tool for the simplified assessment of ancient masonry structures. In Lourenço P.B., Roca P. (Eds.): *Historical Constructions*, Guimarães, 511-520.
- [23] Orduña A., Lourenço P.B. (2003) Cap Model for Limit Analysis and Strengthening of Masonry Structures. *Journal of Structural Engineering*, 129(10), 1367-1376.
- [24] Block, P., Ciblac, T., Ochsendorf, J. A. (2006) Real-time Limit Analysis of Vaulted Masonry Buildings. *Computers and Structures*, 84(29-30), 1841-1852.
- [25] Roca P., Lopez-Almansa F., Miquel J., Hanganu A. (2007) Limit analysis of reinforced masonry vaults. *Engineering Structures* 29, 431-439.
- [26] Milani E., Milani G., Tralli A. (2008) Limit analysis of masonry vaults by means of curved finite elements and homogenization. *International Journal of Solids and Structures*, 45(20), 5258-5288
- [27] Szolomicki, J. P. (2009) Structural behaviour of masonry vaults. In Gürlebeck K. and Könke C. (eds.): *18th Int. Conf. on the Application of Computer Science and Mathematics in Architecture and Civil Engineering*, Weimar, Germany.
- [28] Brencich A., Gambarotta L., Ghia A. (2001) Structural models for the assessment of the masonry dome of the Basilica of S. Maria of Carignano in Genoa. in Lourenço P.B., Roca P. (Eds.): *Proc. 3rd International Seminar on Historical Constructions*, Guimarães, 675-684.
- [29] Block, P., Ochsendorf, J. A., (2005) Interactive Thrust Line Analysis for Masonry Structures. In Mochi G. (ed): *Theory and Practice of Construction: Knowledge, Means, and Models*, Ravenna, Italy, , 473-483.
- [30] Block, P., Ochsendorf, J. (2007) Thrust network analysis: A new methodology for three-dimensional equilibrium. *Journal of the International Association for Shell and Spatial Structures*, 48(3), 167-173.
- [31] Lucchesi, M., Padovani, C., Pasquinelli, G., Zani, N. (2007) Static analysis of masonry vaults, constitutive model and numerical analysis. *J. of Mechanics of Materials and Structures*, 2(2), 221-244.
- [32] Fraternali F. (2010) A thrust network approach to the equilibrium problem of unreinforced masonry vaults via polyhedral stress functions. *Mechanics Research Communications*, 37, 198-204.
- [33] Block P., Lachauer L., Rippmann M. (2010) Validating Thrust Network Analysis using 3D structural models. In: *Proceedings of the International Association for Shell and Spatial Structures (IASSS) Symposium*, Shanghai, China, 2010

Abstract

After discussing the problem of roofing empty spaces by ancient masonry builders, it is found out that curvature and horizontal thrust are the basic elements for masonry to get over long spans. Basic properties of masonry do not allow to rely on tensile strength, and beam behaviour cannot be trusted on. Nevertheless in 2D walls and in double curvature vaults, a particular organization of the vault apparatus can in some instances, through the action of compression and friction, give place to a equilibrium pattern including tension, which explains the unexpected good performance of some walls and cupolas. Anyway, it is recognized that, apart from a few cases, the No-Tension assumption yields a effective model for structural assessment. The theory is briefly illustrated, and its application to vaults is explained in detail, leading to a Monge-Ampere equation ruling the static regime through a membrane stress surface.

Streszczenie

Po przeanalizowaniu problematyki przekryć wznoszonych techniką murarską w dawnych czasach, okazało się, że krzywizna i siły rozporu są głównymi elementami pozwalającymi wykonać murowane konstrukcje ponad dużymi przestrzeniami. Podstawowe właściwości budulca nie gwarantują wytrzymałości na rozciąganie, ani nie dają pewności w kwestii pracy belek. Jednakże w ścianach 2D i sklepieniach o podwójnej krzywiznie, specyficzna konfiguracja sklepienia może w niektórych przypadkach, dzięki działaniu sił ściskających i tarcia, pozwolić na powstanie modelu równowagi obejmującego rozciąganie, co wyjaśnia nadspodziewaną nośność niektórych ścian i kopuł. Ogólnie uznaje się, że z wyjątkiem nielicznych przypadków, założenie braku naprężeń rozciągających daje w efekcie odpowiedni model do oceny konstrukcji. Ta krótko przedstawiona tutaj teoria i jej zastosowanie w przypadku kopuł, zostały szczegółowo wyjaśnione, czego efektem jest równanie Monge-Ampere wyznaczające schemat statyczny w naprężeniu błonowym powierzchni.